Search for physics beyond the standard model in events with two leptons of same sign, missing transverse momentum, and jets in proton-proton collisions at root s=13TeV

Sirunyan, A. M.

2017-09-01

Sirunyan , A M , Eerola , P , Pekkanen , J , Voutilainen , M , Härkönen , J , Järvinen , T , Karimäki , V , Kinnunen , R , Lampén , T , Lassila-Perini , K , Lehti , S , Lindén , T , Luukka , P , Tuominen , E , Tuominiemi , J , Tuovinen , E , Talvitie , J , Tuuva , T & The CMS Collaboration 2017 , ' Search for physics beyond the standard model in events with two leptons of same sign, missing transverse momentum, and jets in proton-proton collisions at root s=13TeV ' , European Physical Journal C. Particles and Fields , vol. 77 , no. 9 , 578 . https://doi.org/10.1140/epjc

http://hdl.handle.net/10138/225933
https://doi.org/10.1140/epjc/s10052-017-5079-z

Eur. Phys. J. C (2017) 77:578
DOI 10.1140/epjc/s10052-017-5079-z

THE EUROPEAN PHYSICAL JOURNAL C

Regular Article - Experimental Physics

Search for physics beyond the standard model in events with two leptons of same sign, missing transverse momentum, and jets in proton–proton collisions at $\sqrt{s} = 13$ TeV

CMS Collaboration*

CERN, 1211 Geneva 23, Switzerland

Received: 24 April 2017 / Accepted: 18 July 2017

Abstract A data sample of events from proton–proton collisions with two isolated same-sign leptons, missing transverse momentum, and jets is studied in a search for signatures of new physics phenomena by the CMS Collaboration at the LHC. The data correspond to an integrated luminosity of 35.9 fb^{-1}, and a center-of-mass energy of 13 TeV. The properties of the events are consistent with expectations from standard model processes, and no excess yield is observed. Exclusion limits at 95% confidence level are set on cross sections for the pair production of gluinos, squarks, and same-sign top quarks, as well as top-quark associated production of a heavy scalar or pseudoscalar boson decaying to top quarks, and on the standard model production of events with four top quarks. The observed lower mass limits are as high as 1500 GeV for gluinos, 830 GeV for bottom squarks. The excluded mass range for heavy (pseudo)scalar bosons is 350–360 (350–410) GeV. Additionally, model-independent limits in several topological regions are provided, allowing for further interpretations of the results.

1 Introduction

Final states with two leptons of same charge, denoted as same-sign (SS) dileptons, are produced rarely by standard model (SM) processes in proton–proton (pp) collisions. Because the SM rates of SS dileptons are low, studies of these final states provide excellent opportunities to search for manifestations of physics beyond the standard model (BSM). Over the last decades, a large number of new physics mechanisms have been proposed to extend the SM and address its shortcomings. Many of these can give rise to potentially large contributions to the SS dilepton signature, e.g., the production of supersymmetric (SUSY) particles [1,2], SS top quarks [3,4], scalar gluons (sgluons) [5,6], heavy scalar bosons of extended Higgs sectors [7,8], Majorana neutrinos [9], and vector-like quarks [10].

In the SUSY framework [11–20], the SS final state can appear in R-parity conserving models through gluino or squark pair production when the decay of each of the pair-produced particles yields one or more W bosons. For example, a pair of gluinos (which are Majorana particles) can give rise to SS charginos and up to four top quarks, yielding signatures with up to four W bosons, as well as jets, b quark jets, and large missing transverse momentum ($E_{\mathrm{T}}^{\mathrm{miss}}$). Similar signatures can also result from the pair production of bottom squarks, subsequently decaying to charginos and top quarks.

While R-parity conserving SUSY models often lead to signatures with large $E_{\mathrm{T}}^{\mathrm{miss}}$, it is also interesting to study final states without significant $E_{\mathrm{T}}^{\mathrm{miss}}$ beyond what is produced by the neutrinos from leptonic W boson decays. For example, some SM and BSM scenarios can lead to the production of SS or multiple top quark pairs, such as the associated production of a heavy (pseudo)scalar, which subsequently decays to a pair of top quarks. This scenario is realized in Type II two Higgs doublet models (2HDM) where associated production with a single top quark or a $\mathrm{t\bar{t}}$ pair can in some cases provide a promising window to probe these heavy (pseudo)scalar bosons [21–23].

This paper extends the search for new physics presented in Ref. [24]. We consider final states with two leptons (electrons and muons) of same charge, two or more hadronic jets, and moderate $E_{\mathrm{T}}^{\mathrm{miss}}$. Compared to searches with zero or one lepton, this final state provides enhanced sensitivity to low-momentum leptons and SUSY models with compressed mass spectra. The results are based on an integrated luminosity corresponding to 35.9 fb^{-1} of $\sqrt{s} = 13$ TeV proton–proton collisions collected with the CMS detector at the CERN LHC. Previous LHC searches in the SS dilepton channel have been performed by the ATLAS [25–27] and CMS [24,28–32] Collaborations. With respect to Ref. [24], the event categoriza-

* e-mail: cms-publication-committee-chair@cern.ch

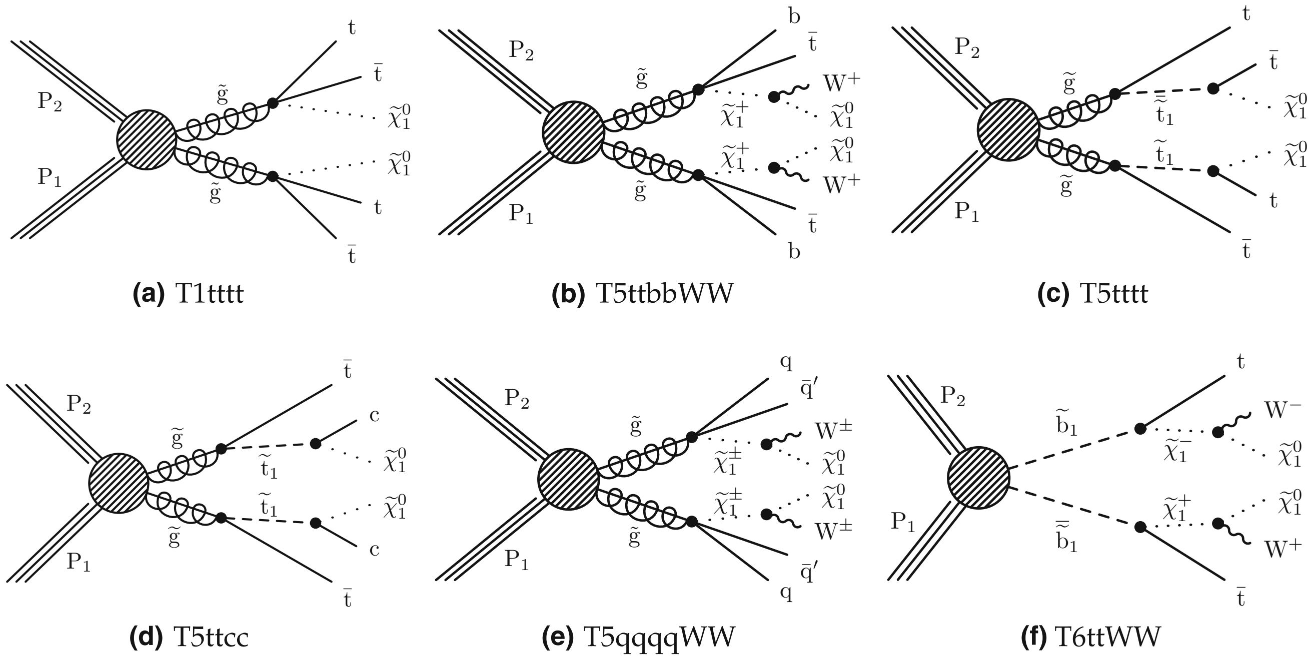

Fig. 1 Diagrams illustrating the simplified SUSY models considered in this analysis

tion is extended to take advantage of the increased integrated luminosity, the estimate of rare SM backgrounds is improved, and the (pseudo)scalar boson interpretation is added.

The results of the search are interpreted in a number of specific BSM models discussed in Sect. 2. In addition, model-independent results are also provided in several kinematic regions to allow for further interpretations. These results are given as a function of hadronic activity and of $E_{\mathrm{T}}^{\mathrm{miss}}$, as well as in a set of inclusive regions with different topologies. The full analysis results are also summarized in a smaller set of exclusive regions to be used in combination with the background correlation matrix to facilitate their reinterpretation.

2 Background and signal simulation

Monte Carlo (MC) simulations are used to estimate SM background contributions and to estimate the acceptance of the event selection for BSM models. The MadGraph5_aMC@NLO 2.2.2 [33–35] and POWHEG v2 [36, 37] next-to-leading order (NLO) generators are used to simulate almost all SM background processes based on the NNPDF3.0 NLO [38] parton distribution functions (PDFs). New physics signal samples, as well as the same-sign $\mathrm{W}^{\pm}\mathrm{W}^{\pm}$ process, are generated with MadGraph5_aMC@NLO at leading order (LO) precision, with up to two additional partons in the matrix element calculations, using the NNPDF3.0 LO [38] PDFs. Parton showering and hadronization, as well as the double-parton scattering production of $\mathrm{W}^{\pm}\mathrm{W}^{\pm}$, are described using the PYTHIA 8.205 generator [39] with the CUETP8M1 tune [40,41]. The Geant4 package [42] is used to model the CMS detector response for background samples, while the CMS fast simulation package [43] is used for signal samples.

To improve on the MadGraph modeling of the multiplicity of additional jets from initial-state radiation (ISR), MadGraph $\mathrm{t\bar{t}}$ MC events are reweighted based on the number of ISR jets (N_J^{ISR}), so as to make the light-flavor jet multiplicity in dilepton $\mathrm{t\bar{t}}$ events agree with the one observed in data. The same reweighting procedure is applied to SUSY MC events. The reweighting factors vary between 0.92 and 0.51 for N_J^{ISR} between 1 and 6. We take one half of the deviation from unity as the systematic uncertainty in these reweighting factors.

The new physics signal models probed by this search are shown in Figs. 1 and 2. In each of the simplified SUSY models [44,45] of Fig. 1, only two or three new particles have masses sufficiently low to be produced on-shell, and the branching fraction for the decays shown are assumed to be 100%. Gluino pair production models giving rise to signatures with up to four b quarks and up to four W bosons are shown in Fig. 1a–e. In these models, the gluino decays to the lightest squark ($\tilde{\mathrm{g}} \to \tilde{\mathrm{q}}\mathrm{q}$), which in turn decays to same-flavor ($\tilde{\mathrm{q}} \to \mathrm{q}\tilde{\chi}_1^0$) or different-flavor ($\tilde{\mathrm{q}} \to \mathrm{q}'\tilde{\chi}_1^{\pm}$) quarks. The chargino decays to a W boson and a neutralino ($\tilde{\chi}_1^{\pm} \to \mathrm{W}^{\pm}\tilde{\chi}_1^0$), where the $\tilde{\chi}_1^0$ escapes detection and is taken to be the lightest SUSY particle (LSP). The first two scenarios considered in Fig. 1a, b include an off-shell third-generation squark ($\tilde{\mathrm{t}}$ or $\tilde{\mathrm{b}}$) leading to the three-body decay of

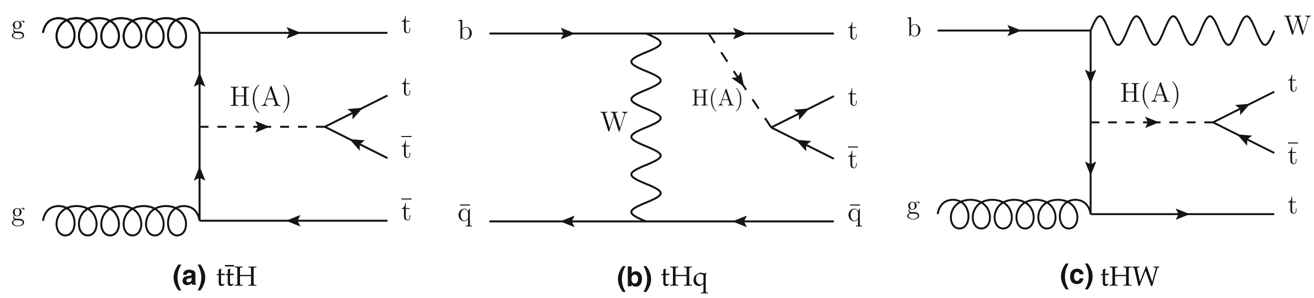

Fig. 2 Diagrams for scalar (pseudoscalar) boson production in association with top quarks

the gluino, $\widetilde{g} \to t\bar{t}\widetilde{\chi}_1^0$ (T1tttt) and $\widetilde{g} \to \bar{t}b\widetilde{\chi}_1^+$ (T5ttbbWW), resulting in events with four W bosons and four b quarks. In the T5ttbbWW model, the mass splitting between chargino and neutralino is set to $m_{\widetilde{\chi}_1^\pm} - m_{\widetilde{\chi}_1^0} = 5\,\text{GeV}$, so that two of the W bosons are produced off-shell and can give rise to low transverse momentum (p_T) leptons. The next two models shown (Fig. 1c, d) include an on-shell top squark with different mass splitting between the $\widetilde{t}$ and the $\widetilde{\chi}_1^0$, and consequently different decay modes: in the T5tttt model the mass splitting is equal to the top quark mass ($m_{\widetilde{t}} - m_{\widetilde{\chi}_1^0} = m_t$), favoring the $\widetilde{t} \to t\widetilde{\chi}_1^0$ decay, while in the T5ttcc model the mass splitting is only 20 GeV, favoring the flavor changing neutral current $\widetilde{t} \to c\widetilde{\chi}_1^0$ decay. In Fig. 1e, the decay proceeds through a virtual light-flavor squark, leading to a three-body decay to $\widetilde{g} \to qq'\widetilde{\chi}_1^\pm$, resulting in a signature with two W bosons and four light-flavor jets. The two W bosons can have the same charge, giving rise to SS dileptons. This model, T5qqqqWW, is studied as a function of the gluino and $\widetilde{\chi}_1^0$ mass, with two different assumptions for the chargino mass: $m_{\widetilde{\chi}_1^\pm} = 0.5(m_{\widetilde{g}}+m_{\widetilde{\chi}_1^0})$, producing mostly on-shell W bosons, and $m_{\widetilde{\chi}_1^\pm} = m_{\widetilde{\chi}_1^0} + 20\,\text{GeV}$, producing off-shell W bosons. Finally, Fig. 1f shows a model of bottom squark production followed by the $\widetilde{b} \to t\widetilde{\chi}_1^\pm$ decay, resulting in two b quarks and four W bosons. This model, T6ttWW, is studied as a function of the $\widetilde{b}$ and $\widetilde{\chi}_1^\pm$ masses, keeping the $\widetilde{\chi}_1^0$ mass at 50 GeV, resulting in two of the W bosons being produced off-shell when the $\widetilde{\chi}_1^\pm$ and $\widetilde{\chi}_1^0$ masses are close. The production cross sections for SUSY models are calculated at NLO plus next-to-leading logarithmic (NLL) accuracy [46–51].

The processes shown in Fig. 2, $t\bar{t}$H, tHq, and tWH, represent the top quark associated production of a scalar (H) or a pseudoscalar (A). The subsequent decay of the (pseudo)scalar to a pair of top quarks then gives rise to final states including a total of three or four top quarks. For the purpose of interpretation, we use LO cross sections for the production of a heavy Higgs boson in the context of the Type II 2HDM of Ref. [23]. The mass of the new particle is varied in the range [350, 550] GeV, where the lower mass boundary is chosen in such a way as to allow the decay of the (pseudo)scalar into on-shell top quarks.

3 The CMS detector and event reconstruction

The central feature of the CMS detector is a superconducting solenoid of 6 m internal diameter, providing a magnetic field of 3.8 T. Within the solenoid volume are a silicon pixel and strip tracker, a lead tungstate crystal electromagnetic calorimeter (ECAL), and a brass and scintillator hadron calorimeter (HCAL), each composed of a barrel and two endcap sections. Forward calorimeters extend the pseudorapidity (η) coverage provided by the barrel and endcap detectors. Muons are measured in gas-ionization detectors embedded in the steel flux-return yoke outside the solenoid. A more detailed description of the CMS detector, together with a definition of the coordinate system used and the relevant kinematic variables, can be found in Ref. [52].

Events of interest are selected using a two-tiered trigger system [53]. The first level (L1), composed of custom hardware processors, uses information from the calorimeters and muon detectors to select events at a rate of around 100 kHz within a time interval of less than 4 μs. The second level, known as the high-level trigger (HLT), consists of a farm of processors running a version of the full event reconstruction software optimized for fast processing, and reduces the event rate to less than 1 kHz before data storage.

Events are processed using the particle-flow (PF) algorithm [54,55], which reconstructs and identifies each individual particle with an optimized combination of information from the various elements of the CMS detector. The energy of photons is directly obtained from the ECAL measurement. The energy of electrons is determined from a combination of the electron momentum at the primary interaction vertex as determined by the tracker, the energy of the corresponding ECAL cluster, and the energy sum of all bremsstrahlung photons spatially compatible with the electron track [56]. The energy of muons is obtained from the curvature of the corresponding track, combining information from the silicon tracker and the muon system [57]. The energy of charged hadrons is determined from a combination of their momentum measured in the tracker and the matching ECAL and HCAL energy deposits, corrected for the response function of the calorimeters to hadronic showers. Finally, the energy of neutral hadrons is obtained from the corresponding corrected ECAL and HCAL energy.

Hadronic jets are clustered from neutral PF candidates and charged PF candidates associated with the primary vertex, using the anti-k_T algorithm [58,59] with a distance parameter $R = \sqrt{(\Delta\eta)^2 + (\Delta\phi)^2}$ of 0.4. Jet momentum is determined as the vectorial sum of all PF candidate momenta in the jet. An offset correction is applied to jet energies to take into account the contribution from additional proton–proton interactions (pileup) within the same or nearby bunch crossings. Jet energy corrections are derived from simulation, and are improved with in situ measurements of the energy balance in dijet and photon+jet events [60,61]. Additional selection criteria are applied to each event to remove spurious jet-like features originating from isolated noise patterns in certain HCAL regions. Jets originating from b quarks are identified (b tagged) using the medium working point of the combined secondary vertex algorithm CSVv2 [62]. The missing transverse momentum vector $\vec{p}_T^{\text{miss}}$ is defined as the projection on the plane perpendicular to the beams of the negative vector sum of the momenta of all reconstructed PF candidates in an event [63]. Its magnitude is referred to as E_T^{miss}. The sum of the transverse momenta of all jets in an event is referred to as H_T.

4 Event selection and search strategy

The event selection and the definition of the signal regions (SRs) follow closely the analysis strategy established in Ref. [24]. With respect to the previous search, the general strategy has remained unchanged. We target, in a generic way, new physics signatures that result in SS dileptons, hadronic activity, and E_T^{miss}, by subdividing the event sample into several SRs sensitive to a variety of new physics models. The number of SRs was increased to take advantage of the larger integrated luminosity. Table 1 summarizes the basic kinematic requirements for jets and leptons (further details, including the lepton identification and isolation requirements, can be found in Ref. [24]).

Events are selected using triggers based on two sets of HLT algorithms, one simply requiring two leptons, and one additionally requiring $H_T > 300$ GeV. The H_T requirement allows for the lepton isolation requirement to be removed and for the lepton p_T thresholds to be set to 8 GeV for both leptons, while in the pure dilepton trigger the leading and subleading leptons are required to have $p_T > 23$ (17) GeV and $p_T > 12$ (8) GeV, respectively, for electrons (muons). Based on these trigger requirements, leptons are classified as high ($p_T > 25$ GeV) and low ($10 < p_T < 25$ GeV) momentum, and three analysis regions are defined: high-high (HH), high-low (HL), and low-low (LL).

The baseline selection used in this analysis requires at least one SS lepton pair with an invariant mass above 8 GeV, at least two jets, and $E_T^{\text{miss}} > 50$ GeV. To reduce Drell–Yan backgrounds, events are rejected if an additional loose lepton forms an opposite-sign same-flavor pair with one of the two SS leptons, with an invariant mass less than 12 GeV or between 76 and 106 GeV. Events passing the baseline selection are then divided into SRs to separate the different background processes and to maximize the sensitivity to signatures with different jet multiplicity (N_{jets}), flavor (N_b), visible and invisible energy (H_T and E_T^{miss}), and lepton momentum spectra (the HH/HL/LL categories mentioned previously). The m_T^{min} variable is defined as the smallest of the transverse masses constructed between $\vec{p}_T^{\text{miss}}$ and each of the leptons. This variable features a cutoff near the W boson mass for processes with only one prompt lepton, so it is used to create SRs where the nonprompt lepton background is negligible. To further improve sensitivity, several regions are split according to the charge of the leptons (++ or −−), taking advantage of the charge asymmetry of SM backgrounds, such as $t\bar{t}W$ or WZ, with a single W boson produced in pp collisions. Only signal regions dominated by such backgrounds and with a sufficient predicted yield are split by charge. In the HH and HL categories, events in the tail regions $H_T > 1125$ GeV or $E_T^{\text{miss}} > 300$ GeV are inclusive in N_{jets}, N_b, and m_T^{min} in order to ensure a reasonable yield of events in these SRs. The exclusive SRs resulting from this classification are defined in Tables 2, 3 and 4.

The lepton reconstruction and identification efficiency is in the range of 45–70% (70–90%) for electrons (muons) with $p_T > 25$ GeV, increasing as a function of p_T and converging to the maximum value for $p_T > 60$ GeV. In the low-momentum regime, $15 < p_T < 25$ GeV for electrons and $10 < p_T < 25$ GeV for muons, the efficiencies are 40% for electrons and 55% for muons. The lepton trigger efficiency for electrons is in the range of 90–98%, converging to the maximum value for $p_T > 30$ GeV, and around 92% for muons. The chosen b tagging working point results in approximately a 70% efficiency for tagging a b quark jet and a <1% mistagging rate for light-flavor jets in $t\bar{t}$ events [62]. The efficiencies of the H_T and E_T^{miss} requirements are mostly determined by the jet energy and E_T^{miss} resolutions, which are discussed in Refs. [60,61,64].

Table 1 Kinematic requirements for leptons and jets. Note that the p_T thresholds to count jets and b-tagged jets are different

Object	p_T (GeV)	$\lvert\eta\rvert$
Electrons	>15	<2.5
Muons	>10	<2.4
Jets	>40	<2.4
b-tagged jets	>25	<2.4

Table 2 Signal region definitions for the HH selection. Regions split by charge are indicated with (++) and (−−). All unlabeled region are included in the SR above them, for example the unlabeled regions between SR3 and SR11 are included in SR3, with the exception of the regions to the right of SR42-45, which are included in those regions

N_b	m_T^{min} (GeV)	E_T^{miss} (GeV)	N_{jets}	$H_T < 300$ GeV	$H_T \in [300, 1125]$ GeV	$H_T \in [1125, 1300]$ GeV	$H_T \in [1300, 1600]$ GeV	$H_T > 1600$ GeV
0	<120	50−200	2−4	SR1	SR2	SR46 (++)/ SR47 (−−)	SR48 (++)/ SR49 (−−)	SR50 (++)/ SR51 (−−)
			≥5	SR3	SR4			
		200−300	2–4		SR5 (++)/ SR6 (−−)			
			≥5		SR7			
	>120	50−200	2–4		SR8 (++)/ SR9 (−−)			
			≥5		SR10			
		200−300	2–4					
			≥5					
1	<120	50−200	2–4	SR11	SR12			
			≥5	SR13 (++)/ SR14 (−−)	SR15 (++)/ SR16 (−−)			
		200−300	2–4		SR17 (++)/ SR18 (−−)			
			≥5		SR19			
	>120	50−200	2–4		SR20 (++)/ SR21 (−−)			
			≥5		SR22			
		200−300	2–4					
			≥5					
2	<120	50−200	2–4	SR23	SR24			
			≥5	SR25 (++)/ SR26 (−−)	SR27 (++)/ SR28 (−−)			
		200−300	2–4		SR29 (++)/ SR30 (−−)			
			≥5		SR31			
	>120	50−200	2–4		SR32 (++)/ SR33 (−−)			
			≥5		SR34			
		200−300	2–4					
			≥5					
≥3	<120	50−200	≥2	SR35 (++)/ SR36 (−−)	SR37 (++)/ SR38 (−−)			
		200−300			SR39			
	>120	50−300	≥2	SR40	SR41			
Inclusive	Inclusive	300−500	≥2	–	SR42 (++)/SR43 (−−)			
		>500		–	SR44 (++)/SR45 (−−)			

5 Backgrounds

Standard model background contributions arise from three sources: processes with prompt SS dileptons, mostly relevant in regions with high E_T^{miss} or H_T; events with a nonprompt lepton, dominating the overall final state; and opposite-sign dilepton events with a charge-misidentified lepton, the smallest contribution. In this paper we use the shorthand "nonprompt leptons" to refer to electrons or muons from the decays of heavy- or light-flavor hadrons, hadrons misidentified as leptons, or electrons from conversions of photons in jets.

Table 3 Signal region definitions for the HL selection. Regions split by charge are indicated with (++) and (−−). All unlabeled region are included in the SR above them, for example the unlabeled regions between SR3 and SR8 are included in SR3, with the exception of the regions to the right of SR34-37, which are included in those regions

N_b	m_T^{min} (GeV)	E_T^{miss} (GeV)	N_{jets}	H_T < 300 GeV	$H_T \in$ [300, 1125] GeV	$H_T \in$ [1125, 1300] GeV	H_T > 1300 GeV
0	<120	50−200	2-4	SR1	SR2	SR38 (++)/ SR39 (−−)	SR40 (++) / SR41 (−−)
			≥5	SR3	SR4		
		200−300	2–4		SR5 (++)/SR6 (−−)		
			≥5		SR7		
1	<120	50−200	2-4	SR8	SR9		
			≥5	SR10 (++)/SR11 (−−)	SR12 (++)/SR13 (−−)		
		200−300	2–4		SR14 (++)/SR15 (−−)		
			≥5		SR16 (++)/SR17 (−−)		
2	<120	50−200	2–4	SR18	SR19		
			≥5	SR20 (++)/SR21 (−−)	SR22 (++)/SR23 (−−)		
		200−300	2–4		SR24 (++)/SR25 (−−)		
			≥5		SR26		
≥3	<120	50−200	≥2	SR27 (++)/SR28 (−−)	SR29 (++)/SR30 (−−)		
		200−300			SR31		
Inclusive	>120	50−300	≥2	SR32	SR33		
Inclusive	Inclusive	300−500	≥2	–	SR34 (++)/SR35 (−−)		
		>500		–	SR36 (++)/SR37 (−−)		

Table 4 Signal region definitions for the LL selection. All SRs in this category require $N_{jets} \geq 2$

N_b	m_T^{min} (GeV)	H_T (GeV)	$E_T^{miss} \in$ [50, 200] GeV	E_T^{miss} > 200 GeV
0	<120	>300	SR1	SR2
1			SR3	SR4
2			SR5	SR6
≥3			SR7	
Inclusive	>120		SR8	

Several categories of SM processes that result in the production of electroweak bosons can give rise to an SS dilepton final state. These include production of multiple bosons in the same event (prompt photons, W, Z, and Higgs bosons), as well as single-boson production in association with top quarks. Among these SM processes, the dominant ones are WZ, $t\bar{t}W$, and $t\bar{t}Z$ production, followed by the $W^{\pm}W^{\pm}$ process. The remaining SM processes are grouped into two categories, "Rare" (including ZZ, WWZ, WZZ, ZZZ, tWZ, tZq, as well as $t\bar{t}t\bar{t}$ and double parton scattering) and "X+γ" (including Wγ, Zγ, $t\bar{t}\gamma$, and tγ). The expected yields from these SM backgrounds are estimated from simulation, accounting for both the theoretical and experimental uncertainties discussed in Sect. 6.

For the WZ and $t\bar{t}Z$ backgrounds, a three-lepton (3L) control region in data is used to scale the simulation, based on a template fit to the distribution of the number of b jets. The 3L control region requires at least two jets, $E_T^{miss} > 30$ GeV, and three leptons, two of which must form an opposite-sign same-flavor pair with an invariant mass within 15 GeV of the Z boson mass. In the fit to data, the normalization and shapes of all the components are allowed to vary according to experimental and theoretical uncertainties. The scale factors obtained from the fit in the phase space of the 3L control region are 1.26 ± 0.09 for the WZ process, and 1.14 ± 0.30 for the $t\bar{t}Z$ process.

The nonprompt lepton background, which is largest for regions with low m_T^{min} and low H_T, is estimated by the "tight-to-loose" method, which was employed in several previous versions of the analysis [28–32], and significantly improved in the latest version [24] to account for the kinematics and flavor of the parent parton of the nonprompt lepton. The tight-to-loose method uses two control regions, the measurement region and the application region. The measurement region consists of a sample of single-lepton events enriched in nonprompt leptons by requirements on E_T^{miss} and transverse mass that suppress the $W \to \ell\nu$ contribution. This sample is used to extract the probability for a nonprompt lepton that satisfies the loose selection to also satisfy the tight selection. This probability (ϵ_{TL}) is calculated as a function of lepton p_T^{corr} (defined below) and η, separately for electrons and muons, and separately for lepton triggers with and without an isolation requirement. The application region is a SS dilepton region where both of the leptons satisfy the loose selection but at least one of them fails the tight selection. This region is subsequently divided into a set of subregions with the exact same kinematic requirements as those in the SRs. Events in the subregions are weighted by a factor $\epsilon_{TL}/(1-\epsilon_{TL})$ for each lepton in the event failing the tight requirement. The nonprompt background in each SR is then estimated as the sum of the event weights in the corresponding subregion. The p_T^{corr} parametrization, where p_T^{corr} is defined as the lepton p_T plus the energy in the isolation cone exceeding the isolation threshold value, is chosen because of its correlation with the parent parton p_T, improving the stability of the ϵ_{TL} values with respect to the sample kinematics. To improve the stability of the ϵ_{TL} values with respect to the flavor of the parent parton, the loose electron selection is adopted. This selection increases the number of nonprompt electrons from the fragmentation and decay of light-flavor partons, resulting in ϵ_{TL} values similar to those from heavy-flavor parent partons.

The prediction from the tight-to-loose method is cross-checked using an alternative method based on the same principle, similar to that described in Ref. [65]. In this cross-check, which aims to remove kinematic differences between measurement and application regions, the measurement region is obtained from SS dilepton events where one of the leptons fails the impact parameter requirement. With respect to the nominal method, the loose lepton definition is adapted to reduce the effect of the correlation between isolation and impact parameter. The predictions of the two methods are found to be consistent within systematic uncertainties.

Charge misidentification of electrons is a small background that can arise from severe bremsstrahlung in the tracker material. Simulation-based studies with tight leptons indicate that the muon charge misidentification probability is negligible, while for electrons it ranges between 10^{-5} and 10^{-3}. The charge misidentification background is estimated from data using an opposite-sign control region for each SS SR, scaling the control region yield by the charge misidentification probability measured in simulation. A low-E_T^{miss} control region, with e^+e^- pairs in the Z boson mass window, is used to cross-check the MC prediction for the misidentification probability, both inclusively and – where the number of events in data allows it – as a function of electron p_T and η.

6 Systematic uncertainties

Several sources of systematic uncertainty affect the predicted yields for signal and background processes, as summarized in Table 5. Experimental uncertainties are based on measurements in data of the trigger efficiency, the lepton identification efficiency, the b tagging efficiency [62], the jet energy scale, and the integrated luminosity [66], as well as on the inelastic cross section value affecting the pileup rate. Theoretical uncertainties related to unknown higher-order effects are estimated by varying simultaneously the factorization and renormalization scales by a factor of two, while uncertainties in the PDFs are obtained using replicas of the NNPDF3.0 set [38].

Experimental and theoretical uncertainties affect both the overall yield (normalization) and the relative population (shape) across SRs, and they are taken into account for all signal samples as well as for the samples used to estimate the main prompt SS dilepton backgrounds: WZ, $t\bar{t}W$, $t\bar{t}Z$, $W^{\pm}W^{\pm}$. For the WZ and $t\bar{t}Z$ backgrounds, the control region fit results are used for the normalization, so these uncertainties are only taken into account for the shape of the backgrounds. For the smallest background samples, Rare and X+γ, a 50% uncertainty is assigned in place of the scale and PDF variations.

Table 5 Summary of the sources of uncertainty and their effect on the yields of different processes in the SRs. The first eight uncertainties are related to experimental and theoretical factors for processes estimated using simulation, while the last four uncertainties are assigned to processes whose yield is estimated from data. The first seven uncertainties also apply to signal samples. Reported values are representative for the most relevant signal regions

Source	Typical uncertainty (%)
Integrated luminosity	2.5
Lepton selection	4–10
Trigger efficiency	2–7
Pileup	0–6
Jet energy scale	1–15
b tagging	1–15
Simulated sample size	1–10
Scale and PDF variations	10–20
WZ (normalization)	12
$t\bar{t}Z$ (normalization)	30
Nonprompt leptons	30–60
Charge misidentification	20

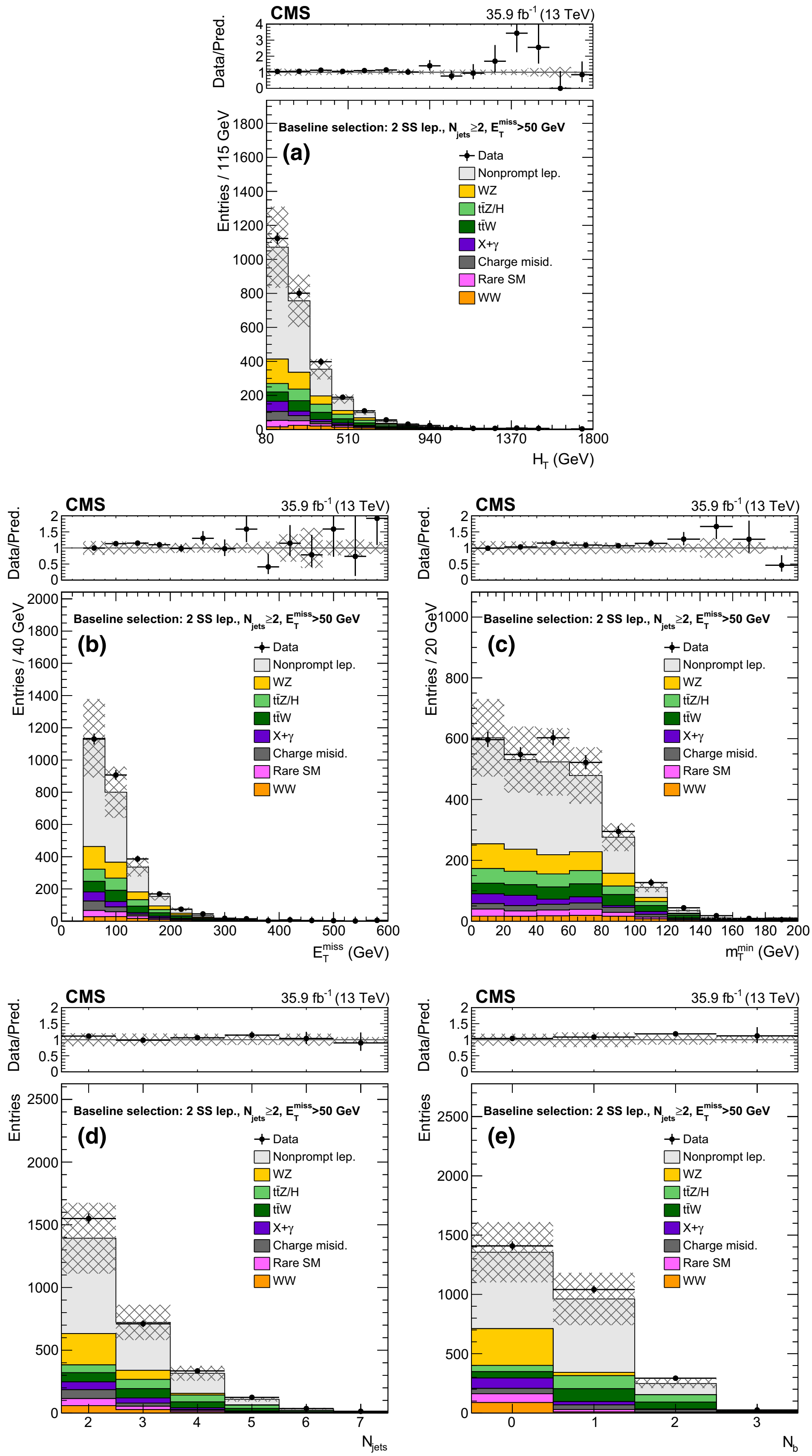

Fig. 3 Distributions of the main analysis variables: H_T (**a**), E_T^{miss} (**b**), m_T^{min} (**c**), N_{jets} (**d**), and N_b (**e**), after the baseline selection requiring a pair of SS leptons, two jets, and $E_T^{miss} > 50$ GeV. The last bin includes the overflow events and the *hatched area* represents the total uncertainty in the background prediction. The *upper panels* show the ratio of the observed event yield to the background prediction

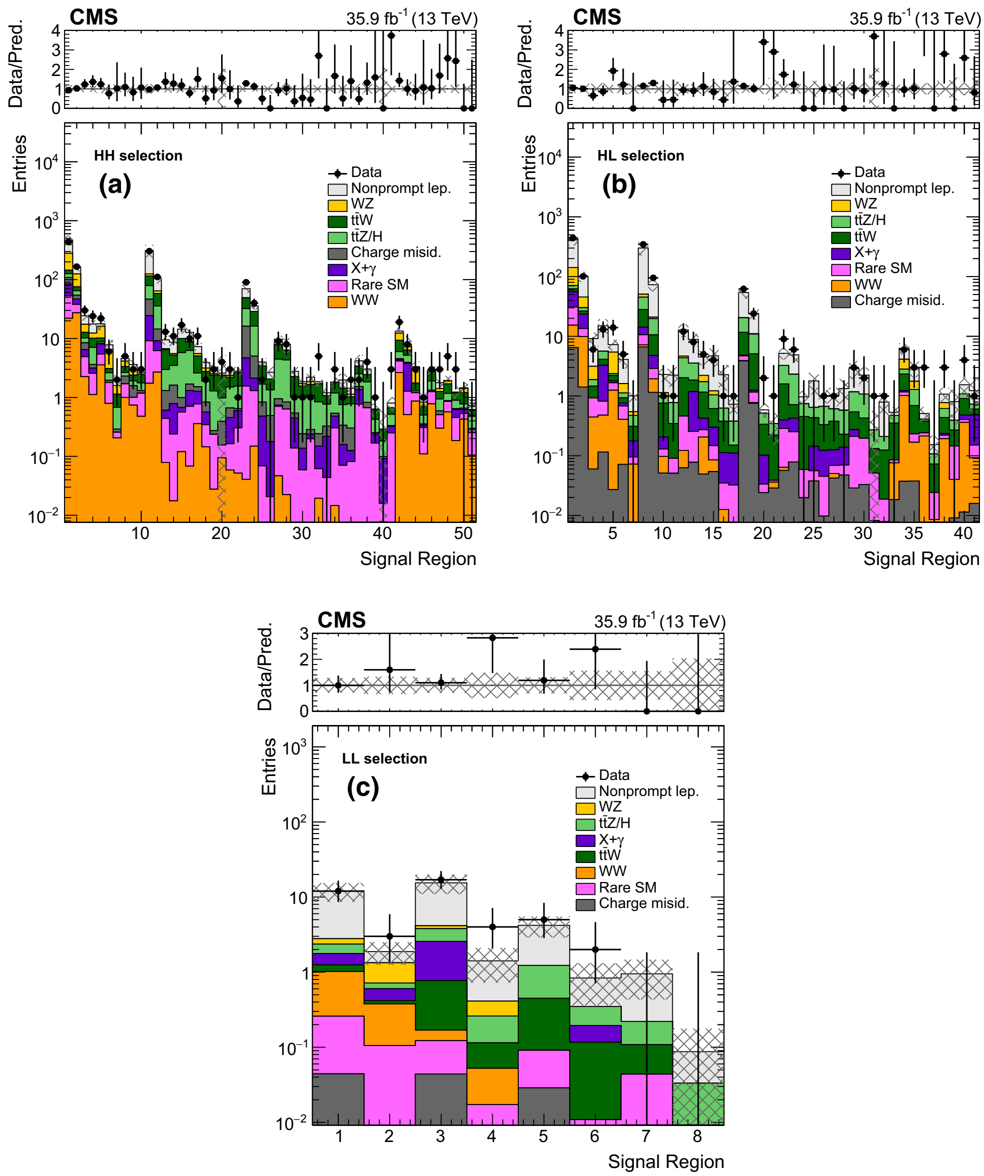

Fig. 4 Event yields in the HH (**a**), HL (**b**), and LL (**c**) signal regions. The *hatched area* represents the total uncertainty in the background prediction. The *upper panels* show the ratio of the observed event yield to the background prediction

The normalization and the shapes of the nonprompt lepton and charge misidentification backgrounds are estimated from control regions in data. In addition to the statistical uncertainties from the control region yields, dedicated systematic uncertainties are associated with the methods used in this estimate. For the nonprompt lepton background, a 30% uncertainty (increased to 60% for electrons with $p_T > 50\,\text{GeV}$) accounts for the performance of the method in simulation and for the differences in the two alternative methods described in Sect. 5. In addition, the uncertainty in the prompt lepton yield in the measurement region, relevant when estimating ϵ_{TL} for high-p_T leptons, results in a 1–30% effect on the estimate. For the charge misidentification background, a 20% uncertainty is assigned to account for possible mismodeling of the charge misidentification rate in simulation.

7 Results and interpretation

A comparison between observed yields and the SM background prediction is shown in Fig. 3 for the kinematic variables used to define the analysis SRs: H_T, E_T^{miss}, m_T^{min}, N_{jets}, and N_b. The distributions are shown after the baseline selection defined in Sect. 4. The full results of the search in each

Table 6 Number of expected background and observed events in different SRs in this analysis

	HH regions		HL regions		LL regions	
	Expected SM	Observed	Expected SM	Observed	Expected SM	Observed
SR1	468 ± 98	435	419 ± 100	442	12.0 ± 3.9	12
SR2	162 ± 25	166	100 ± 20	101	1.88 ± 0.62	3
SR3	24.4 ± 5.4	30	9.2 ± 2.4	6	15.5 ± 4.7	17
SR4	17.6 ± 3.0	24	15.0 ± 4.5	13	1.42 ± 0.69	4
SR5	17.8 ± 3.9	22	7.3 ± 1.5	14	4.2 ± 1.4	5
SR6	7.8 ± 1.5	6	4.1 ± 1.2	5	0.84 ± 0.48	2
SR7	1.96 ± 0.47	2	1.01 ± 0.28	0	0.95 ± 0.52	0
SR8	4.58 ± 0.81	5	300 ± 82	346	0.09 ± 0.07	0
SR9	3.63 ± 0.75	3	73 ± 17	95		
SR10	2.82 ± 0.56	3	2.30 ± 0.61	1		
SR11	313 ± 87	304	2.24 ± 0.87	1		
SR12	104 ± 20	111	12.8 ± 3.3	12		
SR13	9.5 ± 1.9	13	8.9 ± 2.3	8		
SR14	8.7 ± 2.0	11	4.5 ± 1.3	5		
SR15	14.4 ± 2.9	17	4.7 ± 1.6	4		
SR16	12.7 ± 2.6	10	2.3 ± 1.1	1		
SR17	7.3 ± 1.2	11	0.73 ± 0.29	1		
SR18	3.92 ± 0.79	2	54 ± 12	62		
SR19	3.26 ± 0.74	3	23.7 ± 4.9	24		
SR20	2.6 ± 2.7	4	0.59 ± 0.17	2		
SR21	3.02 ± 0.75	3	0.34 ± 0.20	1		
SR22	2.80 ± 0.57	1	5.2 ± 1.2	9		
SR23	70 ± 12	90	4.9 ± 1.4	6		
SR24	35.7 ± 5.9	40	0.97 ± 0.27	0		
SR25	3.99 ± 0.73	2	1.79 ± 0.74	0		
SR26	2.68 ± 0.80	0	1.01 ± 0.27	1		
SR27	9.7 ± 1.8	9	1.03 ± 0.44	1		
SR28	7.9 ± 2.5	8	1.33 ± 0.61	0		
SR29	2.78 ± 0.58	1	2.89 ± 0.99	3		
SR30	1.86 ± 0.38	1	2.24 ± 0.79	2		
SR31	2.20 ± 0.54	1	0.27 ± 0.30	1		
SR32	1.85 ± 0.39	5	0.79 ± 0.33	1		
SR33	1.20 ± 0.32	0	0.53 ± 0.13	0		
SR34	1.81 ± 0.42	3	6.3 ± 1.3	6		
SR35	1.98 ± 0.61	1	2.92 ± 0.87	3		
SR36	1.43 ± 0.37	2	0.51 ± 0.15	3		
SR37	4.2 ± 1.3	2	0.15 ± 0.07	0		
SR38	3.04 ± 0.68	4	1.07 ± 0.33	3		
SR39	0.63 ± 0.17	1	0.81 ± 0.47	0		
SR40	0.29 ± 0.34	0	1.54 ± 0.50	4		
SR41	0.80 ± 0.22	3	1.23 ± 0.53	1		
SR42	13.4 ± 1.9	19				
SR43	8.0 ± 3.0	8				
SR44	3.33 ± 0.74	3				
SR45	0.94 ± 0.26	1				
SR46	2.92 ± 0.50	3				
SR47	1.78 ± 0.42	3				
SR48	1.95 ± 0.39	5				
SR49	1.23 ± 0.30	3				
SR50	1.46 ± 0.31	0				
SR51	0.74 ± 0.18	0				

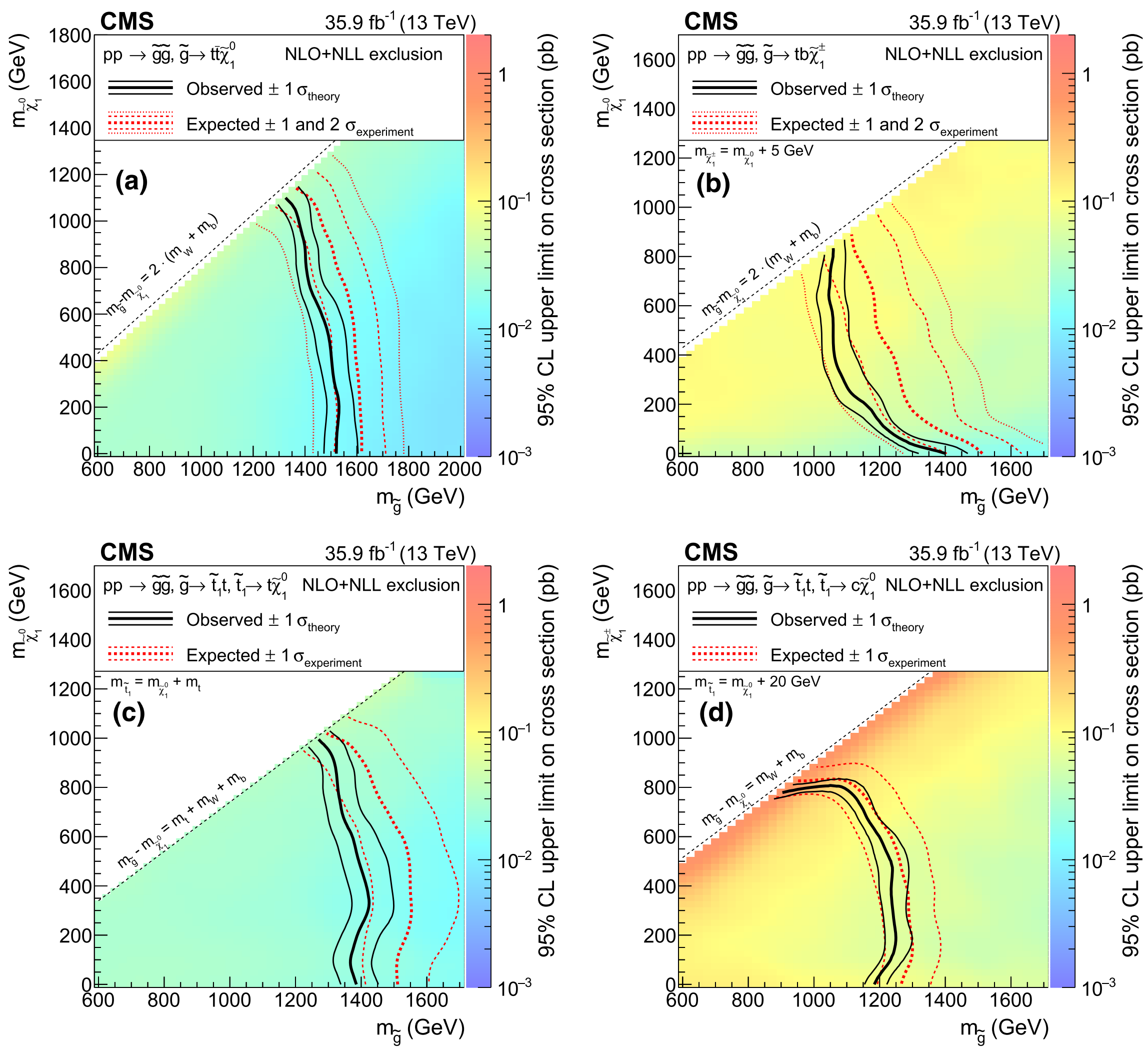

Fig. 5 Exclusion regions at 95% CL in the $m_{\widetilde{\chi}_1^0}$ versus $m_{\widetilde{g}}$ plane for the T1tttt (**a**) and T5ttbbWW (**b**) models, with off-shell third-generation squarks, and the T5tttt (**c**) and T5ttcc (**d**) models, with on-shell third-generation squarks. For the T5ttbbWW model, $m_{\widetilde{\chi}_1^\pm} = m_{\widetilde{\chi}_1^0} + 5\,\text{GeV}$, for the T5tttt model, $m_{\widetilde{t}} - m_{\widetilde{\chi}_1^0} = m_{\mathrm{t}}$, and for the T5ttcc model, $m_{\widetilde{t}} - m_{\widetilde{\chi}_1^0} = 20\,\text{GeV}$ and the decay proceeds through $\widetilde{t} \to c\widetilde{\chi}_1^0$. The *right-hand side color scale* indicates the excluded cross section values for a given point in the SUSY particle mass plane. The *solid*, *black curves* represent the observed exclusion limits assuming the NLO+NLL cross sections [46–51] (*thick line*), or their variations of ±1 standard deviation (*thin lines*). The *dashed*, *red curves* show the expected limits with the corresponding ±1 and ±2 standard deviation experimental uncertainties. Excluded regions are to the left and below the limit curves

SR are shown in Fig. 4 and Table 6. The SM predictions are generally consistent with the data. The largest deviations are seen in HL SR 36 and 38, with a local significance, taking these regions individually or combining them with other regions adjacent in phase space, that does not exceed 2 standard deviations.

These results are used to probe the signal models discussed in Sect. 2: simplified SUSY models, (pseudo)scalar boson production, four top quark production, and SS top quark production. We also interpret the results as model-independent limits as a function of H_{T} and $E_{\mathrm{T}}^{\mathrm{miss}}$. With the exception of the new (pseudo)scalar boson limits, the results can be compared to the previous version of the analysis [24], showing significant improvements due to the increase in the integrated luminosity and the optimization of SR definitions.

To obtain exclusion limits at the 95% confidence level (CL), the results from all SRs – including signal and background uncertainties and their correlations – are combined using an asymptotic formulation of the modified frequentist CL$_s$ criterion [67–70]. When testing a model, all new particles not included in the specific model are considered too heavy to take part in the interaction. To convert cross section limits into mass limits, the signal cross sections specified in Sect. 2 are used.

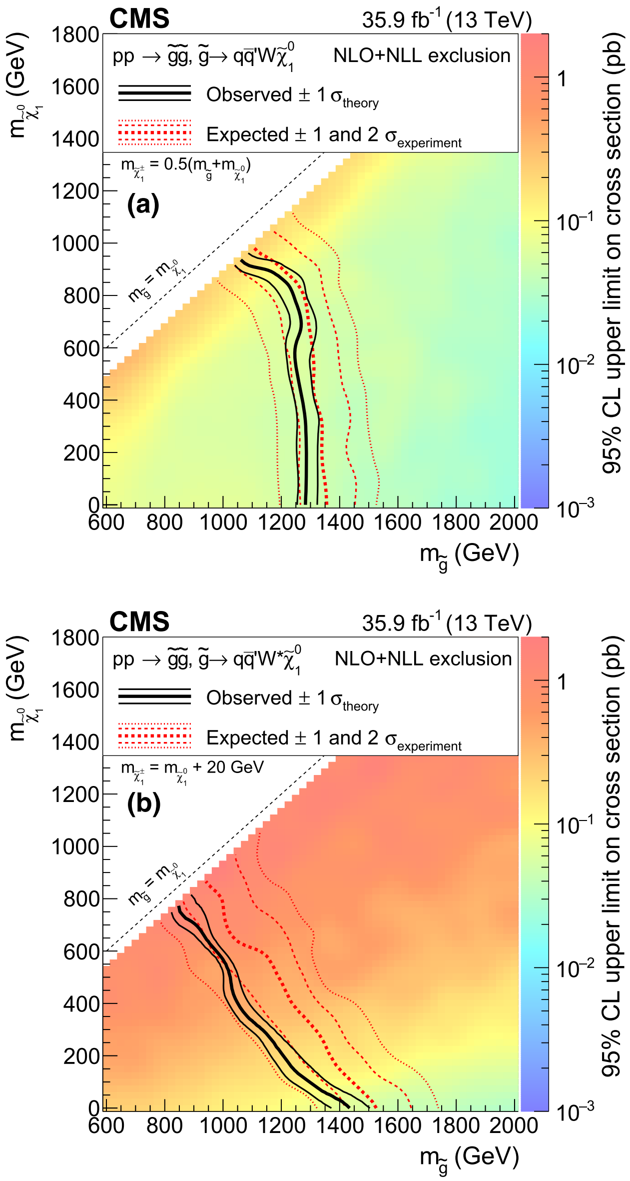

Fig. 6 Exclusion regions at 95% CL in the plane of $m_{\tilde{\chi}_1^0}$ versus $m_{\tilde{g}}$ for the T5qqqqWW model with $m_{\tilde{\chi}_1^\pm} = 0.5(m_{\tilde{g}} + m_{\tilde{\chi}_1^0})$ (**a**) and with $m_{\tilde{\chi}_1^\pm} = m_{\tilde{\chi}_1^0} + 20\,\text{GeV}$ (**b**). The notations are as in Fig. 5

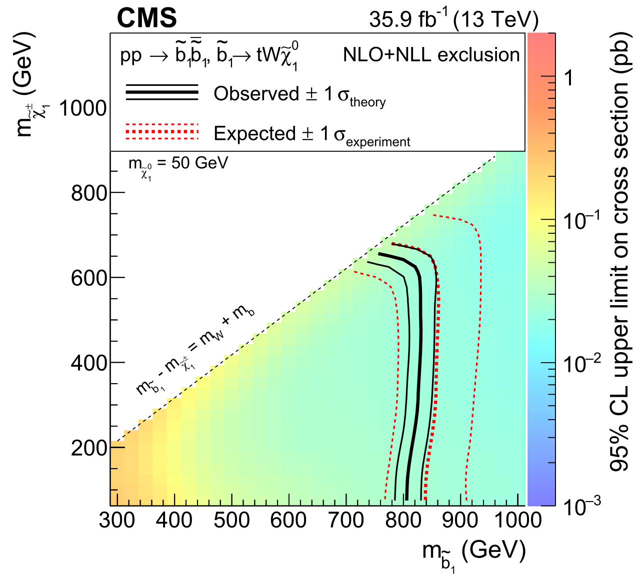

Fig. 7 Exclusion regions at 95% CL in the plane of $m_{\tilde{\chi}_1^\pm}$ versus $m_{\tilde{b}}$ for the T6ttWW model with $m_{\tilde{\chi}_1^0} = 50\,\text{GeV}$. The notations are as in Fig. 5

The observed SUSY cross section limits as a function of the gluino and LSP masses, as well as the observed and expected mass limits for each simplified model, are shown in Fig. 5 for gluino pair production models with each gluino decaying through a chain containing off- or on-shell third-generation squarks. These models, which result in signatures with two or more b quarks and two or more W bosons in the final state, are introduced in Sect. 2 as T1tttt, T5ttbbWW, T5tttt, and T5ttcc. Figure 6 shows the limits for a model of gluino production followed by a decay through off-shell first- or second-generation squarks and a chargino. Two different assumptions are made on the chargino mass, taken to be between that of the gluino and the LSP. These T5qqqqWW models result in no b quarks and either on-shell or off-shell W bosons. Bottom squark pair production followed by a decay through a chargino, T6ttWW, resulting in two b quarks and four W bosons, is shown in Fig. 7. For all of the models probed, the observed limit agrees well with the expected one, extending the reach of the previous analysis by 200–300 GeV and reaching 1.5, 1.1, and 0.83 TeV for gluino, LSP, and bottom squark masses, respectively.

The observed and expected cross section limits on the production of a heavy scalar or a pseudoscalar boson in association with one or two top quarks, followed by its decay to top quarks, are shown in Fig. 8. The limits are compared with the total cross section of the processes described in Sect. 2. The observed limit, which agrees well with the expected one, excludes scalar (pseudoscalar) masses up to 360 (410) GeV.

The SM four top quark production, $pp \to t\bar{t}t\bar{t}$, is normally included among the rare SM backgrounds. When treating this process as signal, its observed (expected) cross section limit is determined to be 42 (27^{+13}_{-8}) fb at 95% CL, to be compared to the SM expectation of $9.2^{+2.9}_{-2.4}$ fb [33]. This is a significant improvement with respect to the observed (expected) limits obtained in the previous version of this analysis, 119 (102^{+57}_{-35}) fb [24], as well as the combination of those results with results from single-lepton and opposite-sign dilepton final states, 69 (71^{+38}_{-24}) fb [71].

The results of the search are also used to set a limit on the production cross section for SS top quark pairs, $\sigma(pp \to tt) + \sigma(pp \to \bar{t}\bar{t})$. The observed (expected) limit, based on the kinematics of a SM $t\bar{t}$ sample and determined using the number of b jets distribution in the baseline region, is 1.2 $(0.76^{+0.3}_{-0.2})$ pb at 95% CL, significantly improved with

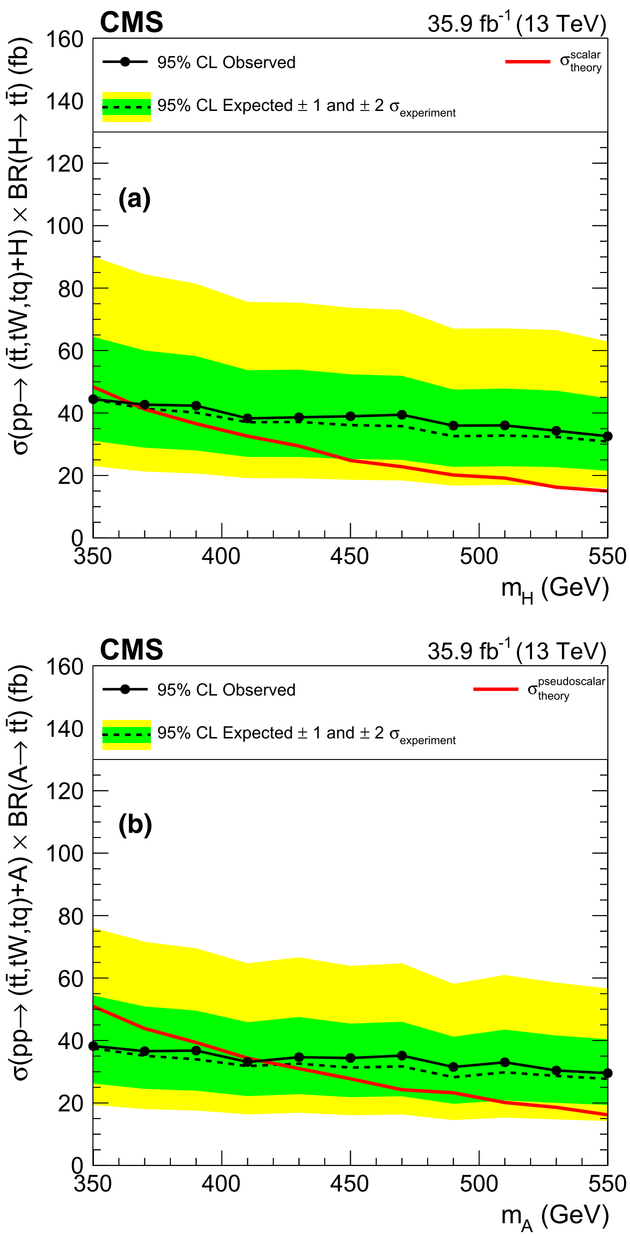

Fig. 8 Limits at 95% CL on the production cross section for heavy scalar (**a**) and pseudoscalar (**b**) boson in association to one or two top quarks, followed by its decay to top quarks, as a function of the (pseudo)scalar mass. The *red line* corresponds to the theoretical cross section in the (pseudo)scalar model

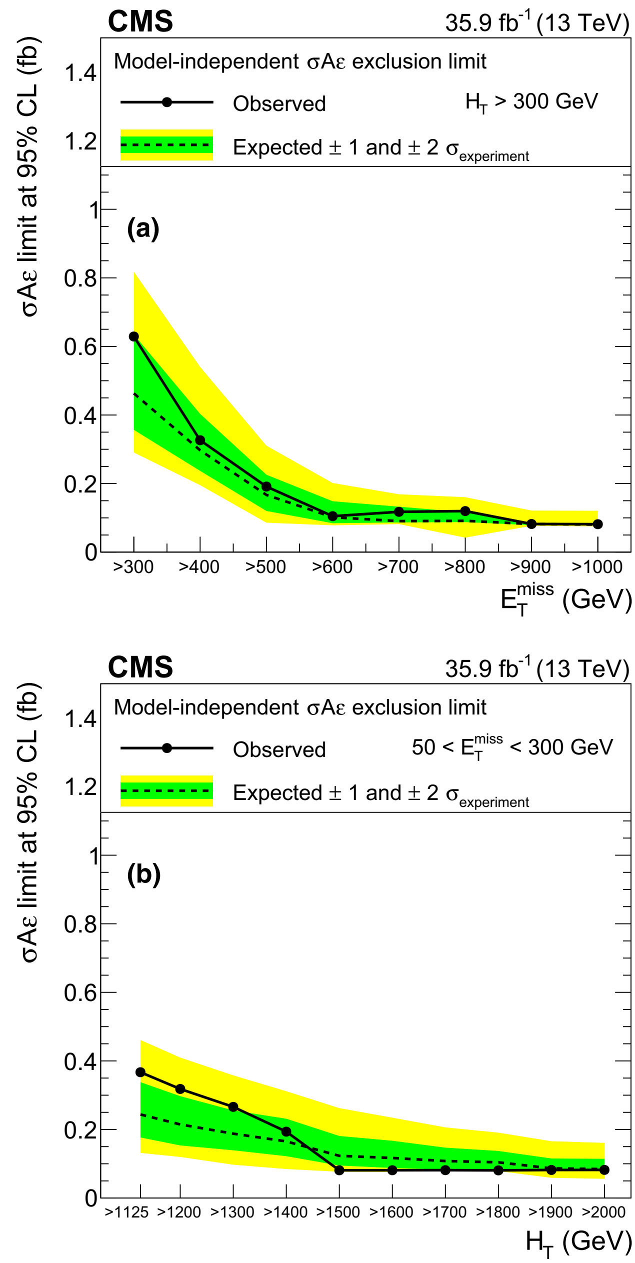

Fig. 9 Limits on the product of cross section, detector acceptance, and selection efficiency, $\sigma\mathcal{A}\epsilon$, for the production of an SS dilepton pair as a function of the E_T^{miss} (**a**) and of H_T (**b**) thresholds

respect to the 1.7 ($1.5^{+0.7}_{-0.4}$) pb observed (expected) limit of the previous analysis [24].

7.1 Model-independent limits and additional results

The yields and background predictions can be used to test additional BSM physics scenarios. To facilitate such reinterpretations, we provide limits on the number of SS dilepton pairs as a function of the E_T^{miss} and H_T thresholds in the kinematic tails, as well as results from a smaller number of inclusive and exclusive signal regions.

The E_T^{miss} and H_T limits are based on combining HH tail SRs, specifically SR42–45 for high E_T^{miss} and SR46–51 for high H_T, and employing the CL$_s$ criterion without the asymptotic formulation as a function of the minimum threshold of each kinematic variable. These limits are presented in Fig. 9 in terms of $\sigma\mathcal{A}\epsilon$, the product of cross section, detector acceptance, and selection efficiency. Where no events are observed, the observed and expected limits reach 0.1 fb, to

Table 7 Inclusive SR definitions, expected background yields, and observed yields, as well the observed 95% CL upper limits on the number of signal events contributing to each region. No uncertainty in the signal acceptance is assumed in calculating these limits. A dash (–) means that the selection is not applied

SR	Leptons	N_{jets}	N_{b}	H_{T} (GeV)	$E_{\text{T}}^{\text{miss}}$ (GeV)	$m_{\text{T}}^{\text{min}}$ (GeV)	SM expected	Observed	$N_{\text{obs,UL}}^{95\%\text{CL}}$
InSR1	HH	≥2	0	≥1200	≥50	–	4.00 ± 0.79	10	12.35
InSR2		≥2	≥2	≥1100	≥50	–	3.63 ± 0.71	4	5.64
InSR3		≥2	0	–	≥450	–	3.72 ± 0.83	4	5.62
InSR4		≥2	≥2	–	≥300	–	3.32 ± 0.81	6	8.08
InSR5		≥2	0	–	≥250	≥120	1.68 ± 0.44	2	4.46
InSR6		≥2	≥2	–	≥150	≥120	3.82 ± 0.76	7	9.06
InSR7		≥2	0	≥900	≥200	–	5.6 ± 1.1	10	10.98
InSR8		≥2	≥2	≥900	≥200	–	5.8 ± 1.3	9	9.77
InSR9		≥7	–	–	≥50	–	10.1 ± 2.7	9	7.39
InSR10		≥4	–	–	≥50	≥120	15.2 ± 3.5	22	16.73
InSR11		≥2	≥3	–	≥50	–	13.3 ± 3.4	17	13.63
InSR12	LL	≥2	0	≥700	≥50	–	3.6 ± 2.5	3	4.91
InSR13		≥2	–	–	≥200	–	4.9 ± 2.9	10	11.76
InSR14		≥5	–	–	≥50	–	7.3 ± 5.5	6	6.37
InSR15		≥2	≥3	–	≥50	–	1.06 ± 0.99	0	2.31

Table 8 Exclusive SR definitions, expected background yields, and observed yields. A dash (–) means that the selection is not applied

SR	Leptons	N_{jets}	N_{b}	$E_{\text{T}}^{\text{miss}}$ (GeV)	H_{T} (GeV)	$m_{\text{T}}^{\text{min}}$ (GeV)	SM expected	Observed
ExSR1	HH	≥2	0	50–300	<1125	<120 for $H_{\text{T}} > 300$	700 ± 130	685
ExSR2		≥2	0	50–300	300–1125	≥120	11.0 ± 2.2	11
ExSR3		≥2	1	50–300	<1125	<120 for $H_{\text{T}} > 300$	477 ± 120	482
ExSR4		≥2	1	50–300	300–1125	≥120	8.4 ± 3.5	8
ExSR5		≥2	2	50–300	<1125	<120 for $H_{\text{T}} > 300$	137 ± 25	152
ExSR6		≥2	2	50–300	300–1125	≥120	4.9 ± 1.2	8
ExSR7		≥2	≥3	50–300	<1125	<120 for $H_{\text{T}} > 300$	11.6 ± 3.1	10
ExSR8		≥2	≥3	50–300	300–1125	≥120	0.8 ± 0.24	3
ExSR9		≥2	–	≥300	≥300	–	25.7 ± 5.4	31
ExSR10		≥2	–	50–300	≥1125	–	10.1 ± 2.2	14
ExSR11	HL	≥2	–	50–300	<1125	<120	1070 ± 250	1167
ExSR12		≥2	–	50–300	<1125	≥120	1.33 ± 0.46	1
ExSR13		≥2	–	≥300	≥300	–	9.9 ± 2.5	12
ExSR14		≥2	–	50–300	≥1125	–	4.7 ± 1.8	8
ExSR15	LL	≥2	–	≥50	≥300	–	37 ± 12	43

be compared with a limit of 1.3 fb obtained in the previous analysis [24].

Results are also provided in Table 7 for a small number of inclusive signal regions, designed based on different topologies and a small number of expected background events. The background expectation, the event count, and the expected BSM yield in any one of these regions can be used to constrain BSM hypotheses in a simple way.

In addition, we define a small number of exclusive signal regions based on integrating over the standard signal regions. Their definitions, as well as the expected and observed yields, are specified in Table 8, while the correlation matrix for the background predictions in these regions is given in Fig. 10. This information can be used to construct a simplified likelihood for models of new physics, as described in Ref. [72].

8 Summary

A sample of same-sign dilepton events produced in proton–proton collisions at 13 TeV, corresponding to an integrated

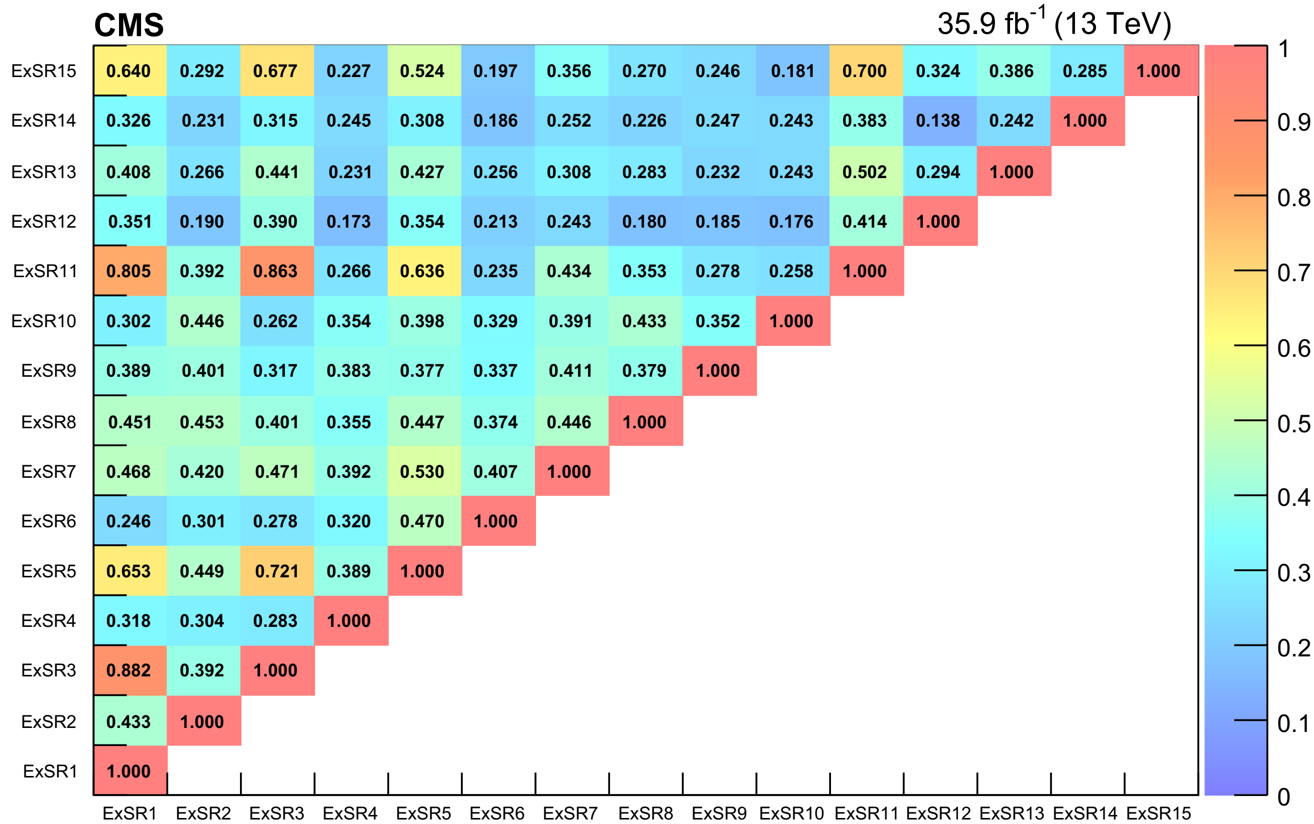

Fig. 10 Correlations between the background predictions in the 15 exclusive regions

luminosity of 35.9 fb^{-1}, has been studied to search for manifestations of physics beyond the standard model. The data are found to be consistent with the standard model expectations, and no excess event yield is observed. The results are interpreted as limits at 95% confidence level on cross sections for the production of new particles in simplified supersymmetric models. Using calculations for these cross sections as functions of particle masses, the limits are turned into lower mass limits that are as high as 1500 GeV for gluinos and 830 GeV for bottom squarks, depending on the details of the model. Limits are also provided on the production of heavy scalar (excluding the mass range 350–360 GeV) and pseudoscalar (350–410 GeV) bosons decaying to top quarks in the context of two Higgs doublet models, as well as on same-sign top quark pair production, and the standard model production of four top quarks. Finally, to facilitate further interpretations of the search, model-independent limits are provided as a function of H_T and E_T^{miss}, together with the background prediction and data yields in a smaller set of signal regions.

Acknowledgements We congratulate our colleagues in the CERN accelerator departments for the excellent performance of the LHC and thank the technical and administrative staffs at CERN and at other CMS institutes for their contributions to the success of the CMS effort. In addition, we gratefully acknowledge the computing centers and personnel of the Worldwide LHC Computing Grid for delivering so effectively the computing infrastructure essential to our analyses. Finally, we acknowledge the enduring support for the construction and operation of the LHC and the CMS detector provided by the following funding agencies: BMWFW and FWF (Austria); FNRS and FWO (Belgium); CNPq, CAPES, FAPERJ, and FAPESP (Brazil); MES (Bulgaria); CERN; CAS, MoST, and NSFC (China); COLCIENCIAS (Colombia); MSES and CSF (Croatia); RPF (Cyprus); SENESCYT (Ecuador); MoER, ERC IUT, and ERDF (Estonia); Academy of Finland, MEC, and HIP (Finland); CEA and CNRS/IN2P3 (France); BMBF, DFG, and HGF (Germany); GSRT (Greece); OTKA and NIH (Hungary); DAE and DST (India); IPM (Iran); SFI (Ireland); INFN (Italy); MSIP and NRF (Republic of Korea); LAS (Lithuania); MOE and UM (Malaysia); BUAP, CINVESTAV, CONACYT, LNS, SEP, and UASLP-FAI (Mexico); MBIE (New Zealand); PAEC (Pakistan); MSHE and NSC (Poland); FCT (Portugal); JINR (Dubna); MON, RosAtom, RAS, RFBR and RAEP (Russia); MESTD (Serbia); SEIDI, CPAN, PCTI and FEDER (Spain); Swiss Funding Agencies (Switzerland); MST (Taipei); ThEPCenter, IPST, STAR, and NSTDA (Thailand); TUBITAK and TAEK (Turkey); NASU and SFFR (Ukraine); STFC (UK); DOE and NSF (USA). Individuals have received support from the Marie-Curie program and the European Research Council and EPLANET (European Union); the Leventis Foundation; the A. P. Sloan Foundation; the Alexander von Humboldt Foundation; the Belgian Federal Science Policy Office; the Fonds pour la Formation à la Recherche dans l'Industrie et dans l'Agriculture (FRIA-Belgium); the Agentschap voor Innovatie door Wetenschap en Technologie (IWT-Belgium); the Ministry of Education, Youth and Sports (MEYS) of the Czech Republic; the Council of Science and Industrial Research, India; the HOMING PLUS program of the Foundation for Polish Science, cofinanced from European Union, Regional Development Fund, the Mobility Plus program of the Ministry of Science and Higher Education, the National Science Center (Poland), contracts Harmonia 2014/14/M/ST2/00428, Opus 2014/13/B/ST2/02543, 2014/15/B/ST2/03998, and 2015/19/B/ST2/02861, Sonata-bis 2012/07/E/ST2/01406; the National Priorities Research Program by Qatar National Research Fund; the Programa Clarín-COFUND del Principado de Asturias; the Thalis and Aristeia programs cofinanced by EU-ESF and the Greek NSRF; the Rachadapisek Sompot Fund for Postdoctoral Fellowship, Chulalongkorn University and the Chulalongkorn Academic into Its 2nd Century Project Advancement Project (Thailand); and the Welch Foundation, contract C-1845.

References

1. R.M. Barnett, J.F. Gunion, H.E. Haber, Discovering supersymmetry with like-sign dileptons. Phys. Lett. B **315**, 349 (1993). doi:10.1016/0370-2693(93)91623-U. arXiv:hep-ph/9306204
2. M. Guchait, D.P. Roy, Like-sign dilepton signature for gluino production at CERN LHC including top quark and Higgs boson effects. Phys. Rev. D **52**, 133 (1995). doi:10.1103/PhysRevD.52.133. arXiv:hep-ph/9412329
3. Y. Bai, Z. Han, Top–antitop and top–top resonances in the dilepton channel at the CERN LHC. JHEP **04**, 056 (2009). doi:10.1088/1126-6708/2009/04/056. arXiv:0809.4487
4. E.L. Berger et al., Top quark forward–backward asymmetry and same-sign top quark pairs. Phys. Rev. Lett. **106**, 201801 (2011). doi:10.1103/PhysRevLett.106.201801. arXiv:1101.5625
5. T. Plehn, T.M.P. Tait, Seeking sgluons. J. Phys. G **36**, 075001 (2009). doi:10.1088/0954-3899/36/7/075001. arXiv:0810.3919
6. S. Calvet, B. Fuks, P. Gris, L. Valery, Searching for sgluons in multitop events at a center-of-mass energy of 8 TeV. JHEP **04**, 043 (2013). doi:10.1007/JHEP04(2013)043. arXiv:1212.3360
7. K.J.F. Gaemers, F. Hoogeveen, Higgs production and decay into heavy flavors with the gluon fusion mechanism. Phys. Lett. B **146**, 347 (1984). doi:10.1016/0370-2693(84)91711-8
8. G.C. Branco et al., Theory and phenomenology of two-Higgs-doublet models. Phys. Rept. **516**, 1 (2012). doi:10.1016/j.physrep.2012.02.002. arXiv:1106.0034
9. F.M.L. Almeida Jr. et al., Same-sign dileptons as a signature for heavy Majorana neutrinos in hadron–hadron collisions. Phys. Lett. B **400**, 331 (1997). doi:10.1016/S0370-2693(97)00143-3. arXiv:hep-ph/9703441
10. R. Contino, G. Servant, Discovering the top partners at the LHC using same-sign dilepton final states. JHEP **06**, 026 (2008). doi:10.1088/1126-6708/2008/06/026. arXiv:0801.1679
11. P. Ramond, Dual theory for free fermions. Phys. Rev. D **3**, 2415 (1971). doi:10.1103/PhysRevD.3.2415
12. Y.A. Gol'fand, E.P. Likhtman, Extension of the algebra of Poincaré group generators and violation of P invariance. JETP Lett. **13**, 323 (1971). http://www.jetpletters.ac.ru/ps/1584/article_24309.pdf
13. A. Neveu, J.H. Schwarz, Factorizable dual model of pions. Nucl. Phys. B **31**, 86 (1971). doi:10.1016/0550-3213(71)90448-2
14. D.V. Volkov, V.P. Akulov, Possible universal neutrino interaction. JETP Lett. **16**, 438 (1972). http://www.jetpletters.ac.ru/ps/1766/article_26864.pdf
15. J. Wess, B. Zumino, A lagrangian model invariant under supergauge transformations. Phys. Lett. B **49**, 52 (1974). doi:10.1016/0370-2693(74)90578-4
16. J. Wess, B. Zumino, Supergauge transformations in four-dimensions. Nucl. Phys. B **70**, 39 (1974). doi:10.1016/0550-3213(74)90355-1
17. P. Fayet, Supergauge invariant extension of the Higgs mechanism and a model for the electron and its neutrino. Nucl. Phys. B **90**, 104 (1975). doi:10.1016/0550-3213(75)90636-7
18. H.P. Nilles, Supersymmetry, supergravity and particle physics. Phys. Rept. **110**, 1 (1984). doi:10.1016/0370-1573(84)90008-5
19. S.P. Martin, in *A Supersymmetry Primer*, ed. by G.L. Kane. Perspectives on Supersymmetry II. Adv. Ser. Direct. High Energy Phys., vol. 21 (World Scientific, Singapore, 2010), p. 1. doi:10.1142/9789814307505_0001
20. G.R. Farrar, P. Fayet, Phenomenology of the production, decay, and detection of new hadronic states associated with supersymmetry. Phys. Lett. B **76**, 575 (1978). doi:10.1016/0370-2693(78)90858-4
21. D. Dicus, A. Stange, S. Willenbrock, Higgs decay to top quarks at hadron colliders. Phys. Lett. B **333**, 126 (1994). doi:10.1016/0370-2693(94)91017-0. arXiv:hep-ph/9404359
22. N. Craig et al., The hunt for the rest of the Higgs bosons. JHEP **06**, 137 (2015). doi:10.1007/JHEP06(2015)137. arXiv:1504.04630
23. N. Craig et al., Heavy Higgs bosons at low tan β: from the LHC to 100 TeV. JHEP **01**, 018 (2017). doi:10.1007/JHEP01(2017)018. arXiv:1605.08744
24. CMS Collaboration, Search for new physics in same-sign dilepton events in proton-proton collisions at $\sqrt{s} = 13$ TeV. Eur. Phys. J. C **76**, 439 (2016). doi:10.1140/epjc/s10052-016-4261-z. arXiv:1605.03171
25. ATLAS Collaboration, Search for gluinos in events with two same-sign leptons, jets and missing transverse momentum with the ATLAS detector in pp collisions at $\sqrt{s} = 7$ TeV. Phys. Rev. Lett. **108**, 241802 (2012). doi:10.1103/PhysRevLett.108.241802. arXiv:1203.5763
26. ATLAS Collaboration, Search for supersymmetry at $\sqrt{s} = 8$ TeV in final states with jets and two same-sign leptons or three leptons with the ATLAS detector. JHEP **06**, 035 (2014). doi:10.1007/JHEP06(2014)035. arXiv:1404.2500
27. Atlas Collaboration, Search for supersymmetry at $\sqrt{s} = 13$ TeV in final states with jets and two same-sign leptons or three leptons with the ATLAS detector. Eur. Phys. J. C **76**, 259 (2016). doi:10.1140/epjc/s10052-016-4095-8. arXiv:1602.09058
28. CMS Collaboration, Search for new physics with same-sign isolated dilepton events with jets and missing transverse energy at the LHC. JHEP **06**, 077 (2011). doi:10.1007/JHEP06(2011)077. arXiv:1104.3168
29. GEANT4 Collaboration, Search for new physics in events with same-sign dileptons and b-tagged jets in pp collisions at $\sqrt{s} = 7$ TeV. JHEP **08**, 110 (2012). doi:10.1007/JHEP08(2012)110. arXiv:1205.3933
30. S. Abdullin et al., Search for new physics with same-sign isolated dilepton events with jets and missing transverse energy. Phys. Rev. Lett. **109**, 071803 (2012). doi:10.1103/PhysRevLett.109.071803. arXiv:1205.6615
31. CMS Collaboration, Search for new physics in events with same-sign dileptons and b jets in pp collisions at $\sqrt{s} = 8$ TeV. JHEP **03**, 037 (2013). doi:10.1007/JHEP03(2013)037. arXiv:1212.6194. **(Erratum: DOI: 10.1007/JHEP07(2013) 041)**
32. CMS Collaboration, Search for new physics in events with same-sign dileptons and jets in pp collisions at 8 TeV. JHEP **01**, 163 (2014). doi:10.1007/JHEP01(2014)163. arXiv:1311.6736
33. J. Alwall et al., The automated computation of tree-level and next-to-leading order differential cross sections, and their matching to parton shower simulations. JHEP **07**, 079 (2014). doi:10.1007/JHEP07(2014)079. arXiv:1405.0301
34. J. Alwall et al., Comparative study of various algorithms forthe merging of parton showers and matrix elements in hadronic

collisions. Eur. Phys. J. C **53**, 473 (2008). doi:10.1140/epjc/s10052-007-0490-5. arXiv:0706.2569
35. R. Frederix, S. Frixione, Merging meets matching in MC@NLO. JHEP **12**, 061 (2012). doi:10.1007/JHEP12(2012)061. arXiv:1209.6215
36. T. Melia, P. Nason, R. Rontsch, G. Zanderighi, W^+W^-, WZ and ZZ production in the POWHEG BOX. JHEP **11**, 078 (2011). doi:10.1007/JHEP11(2011)078. arXiv:1107.5051
37. P. Nason, G. Zanderighi, W^+W^-, WZ and ZZ production in the POWHEG BOX V2. Eur. Phys. J. C **74**, 2702 (2014). doi:10.1140/epjc/s10052-013-2702-5. arXiv:1311.1365
38. NNPDF Collaboration, Parton distributions for the LHC Run II. JHEP **04**, 040 (2015). doi:10.1007/JHEP04(2015)040. arXiv:1410.8849
39. T. Sjöstrand, S. Mrenna, P.Z. Skands, A brief introduction to PYTHIA 8.1. Comput. Phys. Commun. **178**, 852 (2008). doi:10.1016/j.cpc.2008.01.036. arXiv:0710.3820
40. P. Skands, S. Carrazza, J. Rojo, Tuning PYTHIA 8.1: the Monash, tune. Eur. Phys. J. C **74**(2014), 3024 (2013). doi:10.1140/epjc/s10052-014-3024-y. arXiv:1404.5630
41. CMS Collaboration, Event generator tunes obtained from underlying event and multiparton scattering measurements. Eur. Phys. J. C **76**, 155 (2016). doi:10.1140/epjc/s10052-016-3988-x. arXiv:1512.00815
42. GEANT4 Collaboration, A Geant4—a simulation toolkit. Nucl. Instrum. Meth. **506**, 250 (2003). doi:10.1016/S0168-9002(03)01368-8
43. S. Abdullin et al., The fast simulation of the CMS detector at LHC. J. Phys. Conf. Ser. **331**, 032049 (2011). doi:10.1088/1742-6596/331/3/032049
44. D. Alves et al., Simplified models for LHC new physics searches. J. Phys. G **39**, 105005 (2012). doi:10.1088/0954-3899/39/10/105005. arXiv:1105.2838
45. CMS Collaboration, Interpretation of searches for supersymmetry with simplified models. Phys. Rev. D **88**, 052017 (2013). doi:10.1103/PhysRevD.88.052017. arXiv:1301.2175
46. W. Beenakker, R. Höpker, M. Spira, P.M. Zerwas, Squark and gluino production at hadron colliders. Nucl. Phys. B **492**, 51 (1997). doi:10.1016/S0550-3213(97)80027-2. arXiv:hep-ph/9610490
47. A. Kulesza, L. Motyka, Threshold resummation for squark-antisquark and gluino-pair production at the LHC. Phys. Rev. Lett. **102**, 111802 (2009). doi:10.1103/PhysRevLett.102.111802. arXiv:0807.2405
48. A. Kulesza, L. Motyka, Soft gluon resummation for the production of gluino-gluino and squark-antisquark pairs at the LHC. Phys. Rev. D **80**, 095004 (2009). doi:10.1103/PhysRevD.80.095004. arXiv:0905.4749
49. W. Beenakker et al., Soft-gluon resummation for squark and gluino hadroproduction. JHEP **12**, 041 (2009). doi:10.1088/1126-6708/2009/12/041. arXiv:0909.4418
50. W. Beenakker et al., Squark and gluino hadroproduction. Int. J. Mod. Phys. A **26**, 2637 (2011). doi:10.1142/S0217751X11053560. arXiv:1105.1110
51. C. Borschensky et al., Squark and gluino production cross sections in pp collisions at $\sqrt{s}$ = 13, 14, 33 and 100 TeV. Eur. Phys. J. C **74**, 3174 (2014). doi:10.1140/epjc/s10052-014-3174-y. arXiv:1407.5066
52. CMS Collaboration, The CMS experiment at the CERN LHC. JINST **3**, S08004 (2008). doi:10.1088/1748-0221/3/08/S08004
53. CMS Collaboration, The CMS trigger system. JINST **12**, P01020 (2017). doi:10.1088/1748-0221/12/01/P01020. arXiv:1609.02366
54. CMS Collaboration, Particle-flow event reconstruction in CMS and performance for jets, taus, and E_T^{miss}. CMS Physics Analysis Summary CMS-PAS-PFT-09-001 (2009). https://cds.cern.ch/record/1194487
55. CMS Collaboration, Commissioning of the particle-flow event reconstruction with the first LHC collisions recorded in the CMS detector. CMS Physics Analysis Summary CMS-PAS-PFT-10-001 (2010). https://cds.cern.ch/record/1247373
56. CMS Collaboration, Performance of electron reconstruction and selection with the CMS detector in proton–proton collisions at $\sqrt{s}$ = 8 TeV. JINST **10**, P06005 (2015). doi:10.1088/1748-0221/10/06/P06005. arXiv:1502.02701
57. CMS Collaboration, Performance of CMS muon reconstruction in pp collision events at sqrt(s) = 7 TeV. JINST **7**, P10002 (2012). doi:10.1088/1748-0221/7/10/P10002. arXiv:1206.4071
58. M. Cacciari, G.P. Salam, G. Soyez, The anti-k_t jet clustering algorithm. JHEP **04**, 063 (2008). doi:10.1088/1126-6708/2008/04/063. arXiv:0802.1189
59. M. Cacciari, G.P. Salam, G. Soyez, FastJet user manual. Eur. Phys. J. C **72**, 1896 (2012). doi:10.1140/epjc/s10052-012-1896-2. arXiv:1111.6097
60. CMS Collaboration, Determination of jet energy calibration and transverse momentum resolution in CMS. JINST **6**, P11002 (2011). doi:10.1088/1748-0221/6/11/P11002. arXiv:1107.4277
61. CMS Collaboration, Jet energy scale and resolution in the CMS experiment in pp collisions at 8 TeV. JINST **12**, P02014 (2016). doi:10.1088/1748-0221/12/02/P02014. arXiv:1607.03663
62. CMS Collaboration, Identification of b quark jets at the CMS experiment in the LHC Run2. CMS Physics Analysis Summary CMS-PAS-BTV-15-001 (2016). http://cds.cern.ch/record/2138504?ln=en
63. CMS Collaboration, Performance of missing energy reconstruction in 13 TeV pp collision data using the CMS detector. CMS Physics Analysis Summary CMS-PAS-JME-16-001 (2016). http://cds.cern.ch/record/2205284?ln=en
64. CMS Collaboration, Performance of the CMS missing transverse momentum reconstruction in pp data at $\sqrt{s}$ = 8 TeV. JINST **10**, P02006 (2015). doi:10.1088/1748-0221/10/02/P02006. arXiv:1411.0511
65. ATLAS Collaboration, Search for anomalous production of prompt same-sign lepton pairs and pair-produced doubly charged Higgs bosons with $\sqrt{s}$ = 8 TeV pp collisions using the ATLAS detector. JHEP **03**, 041 (2015). doi:10.1007/JHEP03(2015)041. arXiv:1412.0237
66. CMS Collaboration, CMS luminosity measurements for the 2016 data taking period. CMS Physics Analysis Summary CMS-PAS-LUM-17-001 (2017). http://cds.cern.ch/record/2257069?ln=en
67. T. Junk, Confidence level computation for combining searches with small statistics. Nucl. Instrum. Meth. A **434**, 435 (1999). doi:10.1016/S0168-9002(99)00498-2. arXiv:hep-ex/9902006
68. A.L. Read, Presentation of search results: the CL_S technique. J. Phys. G **28**, 2693 (2002). doi:10.1088/0954-3899/28/10/313
69. ATLAS and CMS Collaborations, Procedure for the LHC Higgs boson search combination in summer 2011. ATL-PHYS-PUB-2011-011, CMS NOTE-2011/005, 2011. https://cdsweb.cern.ch/record/1379837
70. G. Cowan, K. Cranmer, E. Gross, O. Vitells, Asymptotic formulae for likelihood-based tests of new physics. Eur. Phys. J. C **71**, 1554 (2011). doi:10.1140/epjc/s10052-011-1554-0. arXiv:1007.1727. **(Erratum: DOI: 10.1140/epjc/s10052-013-2501-z)**
71. CMS Collaboration, Search for standard model production of four top quarks in proton–proton collisions at $\sqrt{s}$ = 13 TeV (2017). Phys. Lett. B **772**, 336 (2017). doi:10.1016/j.physletb.2017.06.064. arXiv:1702.06164
72. CMS Collaboration, Simplified likelihood for the re-interpretation of public CMS results. CMS Note CMS-NOTE-2017-001 (2017). http://cds.cern.ch/record/2242860

CMS Collaboration

Yerevan Physics Institute, Yerevan, Armenia
A. M. Sirunyan, A. Tumasyan

Institut für Hochenergiephysik, Wien, Austria
W. Adam, F. Ambrogi, E. Asilar, T. Bergauer, J. Brandstetter, E. Brondolin, M. Dragicevic, J. Erö, M. Flechl, M. Friedl, R. Frühwirth[1], V. M. Ghete, J. Grossmann, J. Hrubec, M. Jeitler[1], A. König, N. Krammer, I. Krätschmer, D. Liko, T. Madlener, I. Mikulec, E. Pree, D. Rabady, N. Rad, H. Rohringer, J. Schieck[1], R. Schöfbeck, M. Spanring, D. Spitzbart, J. Strauss, W. Waltenberger, J. Wittmann, C. -E. Wulz[1], M. Zarucki

Institute for Nuclear Problems, Minsk, Belarus
V. Chekhovsky, V. Mossolov, J. Suarez Gonzalez

Universiteit Antwerpen, Antwerpen, Belgium
E. A. De Wolf, D. Di Croce, X. Janssen, J. Lauwers, M. Van De Klundert, H. Van Haevermaet, P. Van Mechelen, N. Van Remortel, A. Van Spilbeeck

Vrije Universiteit Brussel, Brussel, Belgium
S. Abu Zeid, F. Blekman, J. D'Hondt, I. De Bruyn, J. De Clercq, K. Deroover, G. Flouris, D. Lontkovskyi, S. Lowette, S. Moortgat, L. Moreels, A. Olbrechts, Q. Python, K. Skovpen, S. Tavernier, W. Van Doninck, P. Van Mulders, I. Van Parijs

Université Libre de Bruxelles, Bruxelles, Belgium
H. Brun, B. Clerbaux, G. De Lentdecker, H. Delannoy, G. Fasanella, L. Favart, R. Goldouzian, A. Grebenyuk, G. Karapostoli, T. Lenzi, J. Luetic, T. Maerschalk, A. Marinov, A. Randle-conde, T. Seva, C. Vander Velde, P. Vanlaer, D. Vannerom, R. Yonamine, F. Zenoni, F. Zhang[2]

Ghent University, Ghent, Belgium
A. Cimmino, T. Cornelis, D. Dobur, A. Fagot, M. Gul, I. Khvastunov, D. Poyraz, C. Roskas, S. Salva, M. Tytgat, W. Verbeke, N. Zaganidis

Université Catholique de Louvain, Louvain-la-Neuve, Belgium
H. Bakhshiansohi, O. Bondu, S. Brochet, G. Bruno, A. Caudron, S. De Visscher, C. Delaere, M. Delcourt, B. Francois, A. Giammanco, A. Jafari, M. Komm, G. Krintiras, V. Lemaitre, A. Magitteri, A. Mertens, M. Musich, K. Piotrzkowski, L. Quertenmont, M. Vidal Marono, S. Wertz

Université de Mons, Mons, Belgium
N. Beliy

Centro Brasileiro de Pesquisas Fisicas, Rio de Janeiro, Brazil
W. L. Aldá Júnior, F. L. Alves, G. A. Alves, L. Brito, M. Correa Martins Junior, C. Hensel, A. Moraes, M. E. Pol, P. Rebello Teles

Universidade do Estado do Rio de Janeiro, Rio de Janeiro, Brazil
E. Belchior Batista Das Chagas, W. Carvalho, J. Chinellato[3], A. Custódio, E. M. Da Costa, G. G. Da Silveira[4], D. De Jesus Damiao, S. Fonseca De Souza, L. M. Huertas Guativa, H. Malbouisson, M. Melo De Almeida, C. Mora Herrera, L. Mundim, H. Nogima, A. Santoro, A. Sznajder, E. J. Tonelli Manganote[3], F. Torres Da E Silva De Araujo, A. Vilela Pereira

Universidade Estadual Paulista [a], Universidade Federal do ABC [b], São Paulo, Brazil
S. Ahuja[a], C. A. Bernardes[a], T. R. Fernandez Perez Tomei[a], E. M. Gregores[b], P. G. Mercadante[b], C. S. Moon[a], S. F. Novaes[a], Sandra S. Padula[a], D. Romero Abad[b], J. C. Ruiz Vargas[a]

Institute for Nuclear Research and Nuclear Energy, Sofia, Bulgaria
A. Aleksandrov, R. Hadjiiska, P. Iaydjiev, M. Misheva, M. Rodozov, M. Shopova, S. Stoykova, G. Sultanov

University of Sofia, Sofia, Bulgaria
A. Dimitrov, I. Glushkov, L. Litov, B. Pavlov, P. Petkov

Beihang University, Beijing, China
W. Fang[5], X. Gao[5]

Institute of High Energy Physics, Beijing, China
M. Ahmad, J. G. Bian, G. M. Chen, H. S. Chen, M. Chen, Y. Chen, C. H. Jiang, D. Leggat, Z. Liu, F. Romeo, S. M. Shaheen, A. Spiezia, J. Tao, C. Wang, Z. Wang, E. Yazgan, H. Zhang, J. Zhao

State Key Laboratory of Nuclear Physics and Technology, Peking University, Beijing, China
Y. Ban, G. Chen, Q. Li, S. Liu, Y. Mao, S. J. Qian, D. Wang, Z. Xu

Universidad de Los Andes, Bogota, Colombia
C. Avila, A. Cabrera, L. F. Chaparro Sierra, C. Florez, C. F. González Hernández, J. D. Ruiz Alvarez

University of Split, Faculty of Electrical Engineering, Mechanical Engineering and Naval Architecture, Split, Croatia
B. Courbon, N. Godinovic, D. Lelas, I. Puljak, P. M. Ribeiro Cipriano, T. Sculac

University of Split, Faculty of Science, Split, Croatia
Z. Antunovic, M. Kovac

Institute Rudjer Boskovic, Zagreb, Croatia
V. Brigljevic, D. Ferencek, K. Kadija, B. Mesic, T. Susa

University of Cyprus, Nicosia, Cyprus
M. W. Ather, A. Attikis, G. Mavromanolakis, J. Mousa, C. Nicolaou, F. Ptochos, P. A. Razis, H. Rykaczewski

Charles University, Prague, Czech Republic
M. Finger[6], M. Finger Jr.[6]

Universidad San Francisco de Quito, Quito, Ecuador
E. Carrera Jarrin

Academy of Scientific Research and Technology of the Arab Republic of Egypt, Egyptian Network of High Energy Physics, Cairo, Egypt
Y. Assran[7,8], S. Elgammal[8], A. Mahrous[9]

National Institute of Chemical Physics and Biophysics, Tallinn, Estonia
R. K. Dewanjee, M. Kadastik, L. Perrini, M. Raidal, A. Tiko, C. Veelken

Department of Physics, University of Helsinki, Helsinki, Finland
P. Eerola, J. Pekkanen, M. Voutilainen

Helsinki Institute of Physics, Helsinki, Finland
J. Härkönen, T. Järvinen, V. Karimäki, R. Kinnunen, T. Lampén, K. Lassila-Perini, S. Lehti, T. Lindén, P. Luukka, E. Tuominen, J. Tuominiemi, E. Tuovinen

Lappeenranta University of Technology, Lappeenranta, Finland
J. Talvitie, T. Tuuva

IRFU, CEA, Université Paris-Saclay, Gif-sur-Yvette, France
M. Besancon, F. Couderc, M. Dejardin, D. Denegri, J. L. Faure, F. Ferri, S. Ganjour, S. Ghosh, A. Givernaud, P. Gras, G. Hamel de Monchenault, P. Jarry, I. Kucher, E. Locci, M. Machet, J. Malcles, G. Negro, J. Rander, A. Rosowsky, M. Ö. Sahin, M. Titov

Laboratoire Leprince-Ringuet, Ecole polytechnique, CNRS/IN2P3, Université Paris-Saclay, Palaiseau, France
A. Abdulsalam, I. Antropov, S. Baffioni, F. Beaudette, P. Busson, L. Cadamuro, C. Charlot, O. Davignon, R. Granier de Cassagnac, M. Jo, S. Lisniak, A. Lobanov, J. Martin Blanco, M. Nguyen, C. Ochando, G. Ortona, P. Paganini, P. Pigard, S. Regnard, R. Salerno, J. B. Sauvan, Y. Sirois, A. G. Stahl Leiton, T. Strebler, Y. Yilmaz, A. Zabi

Université de Strasbourg, CNRS, IPHC UMR 7178, 67000 Strasbourg, France
J.-L. Agram[10], J. Andrea, D. Bloch, J.-M. Brom, M. Buttignol, E. C. Chabert, N. Chanon, C. Collard, E. Conte[10], X. Coubez, J.-C. Fontaine[10], D. Gelé, U. Goerlach, M. Jansová, A.-C. Le Bihan, N. Tonon, P. Van Hove

Centre de Calcul de l'Institut National de Physique Nucleaire et de Physique des Particules, CNRS/IN2P3 Villeurbanne, France
S. Gadrat

Université de Lyon, Université Claude Bernard Lyon 1, CNRS-IN2P3, Institut de Physique Nucléaire de Lyon, Villeurbanne, France
S. Beauceron, C. Bernet, G. Boudoul, R. Chierici, D. Contardo, P. Depasse, H. El Mamouni, J. Fay, L. Finco, S. Gascon, M. Gouzevitch, G. Grenier, B. Ille, F. Lagarde, I. B. Laktineh, M. Lethuillier, L. Mirabito, A. L. Pequegnot, S. Perries, A. Popov[11], V. Sordini, M. Vander Donckt, S. Viret

Georgian Technical University, Tbilisi, Georgia
A. Khvedelidze[6]

Tbilisi State University, Tbilisi, Georgia
Z. Tsamalaidze[6]

RWTH Aachen University, I. Physikalisches Institut, Aachen, Germany
C. Autermann, S. Beranek, L. Feld, M. K. Kiesel, K. Klein, M. Lipinski, M. Preuten, C. Schomakers, J. Schulz, T. Verlage

RWTH Aachen University, III. Physikalisches Institut A, Aachen, Germany
A. Albert, M. Brodski, E. Dietz-Laursonn, D. Duchardt, M. Endres, M. Erdmann, S. Erdweg, T. Esch, R. Fischer, A. Güth, M. Hamer, T. Hebbeker, C. Heidemann, K. Hoepfner, S. Knutzen, M. Merschmeyer, A. Meyer, P. Millet, S. Mukherjee, M. Olschewski, K. Padeken, T. Pook, M. Radziej, H. Reithler, M. Rieger, F. Scheuch, D. Teyssier, S. Thüer

RWTH Aachen University, III. Physikalisches Institut B, Aachen, Germany
G. Flügge, B. Kargoll, T. Kress, A. Künsken, J. Lingemann, T. Müller, A. Nehrkorn, A. Nowack, C. Pistone, O. Pooth, A. Stahl[12]

Deutsches Elektronen-Synchrotron, Hamburg, Germany
M. Aldaya Martin, T. Arndt, C. Asawatangtrakuldee, K. Beernaert, O. Behnke, U. Behrens, A. A. Bin Anuar, K. Borras[13], V. Botta, A. Campbell, P. Connor, C. Contreras-Campana, F. Costanza, C. Diez Pardos, G. Eckerlin, D. Eckstein, T. Eichhorn, E. Eren, E. Gallo[14], J. Garay Garcia, A. Geiser, A. Gizhko, J. M. Grados Luyando, A. Grohsjean, P. Gunnellini, A. Harb, J. Hauk, M. Hempel[15], H. Jung, A. Kalogeropoulos, M. Kasemann, J. Keaveney, C. Kleinwort, I. Korol, D. Krücker, W. Lange, A. Lelek, T. Lenz, J. Leonard, K. Lipka, W. Lohmann[15], R. Mankel, I.-A. Melzer-Pellmann, A. B. Meyer, G. Mittag, J. Mnich, A. Mussgiller, E. Ntomari, D. Pitzl, R. Placakyte, A. Raspereza, B. Roland, M. Savitskyi, P. Saxena, R. Shevchenko, S. Spannagel, N. Stefaniuk, G. P. Van Onsem, R. Walsh, Y. Wen, K. Wichmann, C. Wissing, O. Zenaiev

University of Hamburg, Hamburg, Germany
S. Bein, V. Blobel, M. Centis Vignali, A. R. Draeger, T. Dreyer, E. Garutti, D. Gonzalez, J. Haller, M. Hoffmann, A. Junkes, A. Karavdina, R. Klanner, R. Kogler, N. Kovalchuk, S. Kurz, T. Lapsien, I. Marchesini, D. Marconi, M. Meyer, M. Niedziela, D. Nowatschin, F. Pantaleo[12], T. Peiffer, A. Perieanu, C. Scharf, P. Schleper, A. Schmidt, S. Schumann, J. Schwandt, J. Sonneveld, H. Stadie, G. Steinbrück, F. M. Stober, M. Stöver, H. Tholen, D. Troendle, E. Usai, L. Vanelderen, A. Vanhoefer, B. Vormwald

Institut für Experimentelle Kernphysik, Karlsruhe, Germany
M. Akbiyik, C. Barth, S. Baur, E. Butz, R. Caspart, T. Chwalek, F. Colombo, W. De Boer, A. Dierlamm, B. Freund, R. Friese, M. Giffels, A. Gilbert, D. Haitz, F. Hartmann[12], S. M. Heindl, U. Husemann, F. Kassel[12], S. Kudella, H. Mildner, M. U. Mozer, Th. Müller, M. Plagge, G. Quast, K. Rabbertz, M. Schröder, I. Shvetsov, G. Sieber, H. J. Simonis, R. Ulrich, S. Wayand, M. Weber, T. Weiler, S. Williamson, C. Wöhrmann, R. Wolf

Institute of Nuclear and Particle Physics (INPP), NCSR Demokritos, Aghia Paraskevi, Greece
G. Anagnostou, G. Daskalakis, T. Geralis, V. A. Giakoumopoulou, A. Kyriakis, D. Loukas, I. Topsis-Giotis

National and Kapodistrian University of Athens, Athens, Greece
S. Kesisoglou, A. Panagiotou, N. Saoulidou

University of Ioánnina, Ioánnina, Greece
I. Evangelou, C. Foudas, P. Kokkas, N. Manthos, I. Papadopoulos, E. Paradas, J. Strologas, F. A. Triantis

MTA-ELTE Lendület CMS Particle and Nuclear Physics Group, Eötvös Loránd University, Budapest, Hungary
M. Csanad, N. Filipovic, G. Pasztor

Wigner Research Centre for Physics, Budapest, Hungary
G. Bencze, C. Hajdu, D. Horvath[16], Hunyadi, F. Sikler, V. Veszpremi, G. Vesztergombi[17], A. J. Zsigmond

Institute of Nuclear Research ATOMKI, Debrecen, Hungary
N. Beni, S. Czellar, J. Karancsi[18], A. Makovec, J. Molnar, Z. Szillasi

Institute of Physics, University of Debrecen, Debrecen, Hungary
M. Bartók[17], P. Raics, Z. L. Trocsanyi, B. Ujvari

Indian Institute of Science (IISc), Bangalore, India
S. Choudhury, J. R. Komaragiri

National Institute of Science Education and Research, Bhubaneswar, India
S. Bahinipati[19], S. Bhowmik, P. Mal, K. Mandal, A. Nayak[20], D. K. Sahoo[19], N. Sahoo, S. K. Swain

Panjab University, Chandigarh, India
S. Bansal, S. B. Beri, V. Bhatnagar, R. Chawla, N. Dhingra, U. Bhawandeep, A. K. Kalsi, A. Kaur, M. Kaur, R. Kumar, P. Kumari, A. Mehta, J. B. Singh, G. Walia

University of Delhi, Delhi, India
Ashok Kumar, Aashaq Shah, A. Bhardwaj, S. Chauhan, B. C. Choudhary, R. B. Garg, S. Keshri, A. Kumar, S. Malhotra, M. Naimuddin, K. Ranjan, R. Sharma, V. Sharma

Saha Institute of Nuclear Physics, Kolkata, India
R. Bhardwaj, R. Bhattacharya, S. Bhattacharya, S. Dey, S. Dutt, S. Dutta, S. Ghosh, N. Majumdar, A. Modak, K. Mondal, S. Mukhopadhyay, S. Nandan, A. Purohit, A. Roy, D. Roy, S. Roy Chowdhury, S. Sarkar, M. Sharan, S. Thakur

Indian Institute of Technology Madras, Madras, India
P. K. Behera

Bhabha Atomic Research Centre, Mumbai, India
R. Chudasama, D. Dutta, V. Jha, V. Kumar, A. K. Mohanty[12], P. K. Netrakanti, L. M. Pant, P. Shukla, A. Topkar

Tata Institute of Fundamental Research-A, Mumbai, India
T. Aziz, S. Dugad, B. Mahakud, S. Mitra, G. B. Mohanty, B. Parida, N. Sur, B. Sutar

Tata Institute of Fundamental Research-B, Mumbai, India
S. Banerjee, S. Bhattacharya, S. Chatterjee, P. Das, M. Guchait, Sa. Jain, S. Kumar, M. Maity[21], G. Majumder, K. Mazumdar, T. Sarkar[21], N. Wickramage[22]

Indian Institute of Science Education and Research (IISER), Pune, India
S. Chauhan, S. Dube, V. Hegde, A. Kapoor, K. Kothekar, S. Pandey, A. Rane, S. Sharma

Institute for Research in Fundamental Sciences (IPM), Tehran, Iran
S. Chenarani[23], E. Eskandari Tadavani, S. M. Etesami[23], M. Khakzad, M. Mohammadi Najafabadi, M. Naseri, S. Paktinat Mehdiabadi[24], F. Rezaei Hosseinabadi, B. Safarzadeh[25], M. Zeinali

University College Dublin, Dublin, Ireland
M. Felcini, M. Grunewald

INFN Sezione di Bari [a], Università di Bari [b], Politecnico di Bari [c], Bari, Italy
M. Abbrescia[a,b], C. Calabria[a,b], C. Caputo[a,b], A. Colaleo[a], D. Creanza[a,c], L. Cristella[a,b], N. De Filippis[a,c], M. De Palma[a,b], F. Errico[a,b], L. Fiore[a], G. Iaselli[a,c], G. Maggi[a,c], M. Maggi[a], G. Miniello[a,b], S. My[a,b], S. Nuzzo[a,b], A. Pompili[a,b], G. Pugliese[a,c], R. Radogna[a,b], A. Ranieri[a], G. Selvaggi[a,b], A. Sharma[a], L. Silvestris[a,12], R. Venditti[a], P. Verwilligen[a]

INFN Sezione di Bologna [a], Università di Bologna [b], Bologna, Italy
G. Abbiendi[a], C. Battilana, D. Bonacorsi[a,b], S. Braibant-Giacomelli[a,b], L. Brigliadori[a,b], R. Campanini[a,b], P. Capiluppi[a,b], A. Castro[a,b], F. R. Cavallo[a], S. S. Chhibra[a,b], G. Codispoti[a,b], M. Cuffiani[a,b], G. M. Dallavalle[a], F. Fabbri[a], A. Fanfani[a,b], D. Fasanella[a,b], P. Giacomelli[a], L. Guiducci[a,b], S. Marcellini[a], G. Masetti[a], F. L. Navarria[a,b], A. Perrotta[a], A. M. Rossi[a,b], T. Rovelli[a,b], G. P. Siroli[a,b], N. Tosi[a,b,12]

INFN Sezione di Catania [a], Università di Catania [b], Catania, Italy
S. Albergo[a,b], S. Costa[a,b], A. Di Mattia[a], F. Giordano[a,b], R. Potenza[a,b], A. Tricomi[a,b], C. Tuve[a,b]

INFN Sezione di Firenze [a], Università di Firenze [b], Firenze, Italy
G. Barbagli[a], K. Chatterjee[a,b], V. Ciulli[a,b], C. Civinini[a], R. D'Alessandro[a,b], E. Focardi[a,b], P. Lenzi[a,b], M. Meschini[a], S. Paoletti[a], L. Russo[a,26], G. Sguazzoni[a], D. Strom[a], L. Viliani[a,b,12]

INFN Laboratori Nazionali di Frascati, Frascati, Italy
L. Benussi, S. Bianco, F. Fabbri, D. Piccolo, F. Primavera[12]

INFN Sezione di Genova [a], Università di Genova [b], Genova, Italy
V. Calvelli[a,b], F. Ferro[a], E. Robutti[a], S. Tosi[a,b]

INFN Sezione di Milano-Bicocca [a], Università di Milano-Bicocca [b], Milan, Italy
L. Brianza[a,b], F. Brivio[a,b], V. Ciriolo[a,b], M. E. Dinardo[a,b], S. Fiorendi[a,b], S. Gennai[a], A. Ghezzi[a,b], P. Govoni[a,b], M. Malberti[a,b], S. Malvezzi[a], R. A. Manzoni[a,b], D. Menasce[a], L. Moroni[a], M. Paganoni[a,b], K. Pauwels[a,b], D. Pedrini[a], S. Pigazzini[a,b,27], S. Ragazzi[a,b], T. Tabarelli de Fatis[a,b]

INFN Sezione di Napoli [a], Università di Napoli 'Federico II' [b], Naples, Italy, Università della Basilicata [c], Potenza, Italy, Università G. Marconi [d], Rome, Italy
S. Buontempo[a], N. Cavallo[a,c], S. Di Guida[a,d,12], M. Esposito[a,b], F. Fabozzi[a,c], F. Fienga[a,b], A. O. M. Iorio[a,b], W. A. Khan[a], G. Lanza[a], L. Lista[a], S. Meola[a,d,12], P. Paolucci[a,12], C. Sciacca[a,b], F. Thyssen[a]

INFN Sezione di Padova [a], Università di Padova [b], Padoa, Italy, Università di Trento [c], Trento, Italy
P. Azzi[a,12], N. Bacchetta[a], L. Benato[a,b], D. Bisello[a,b], A. Boletti[a,b], R. Carlin[a,b], A. Carvalho Antunes De Oliveira[a,b], P. Checchia[a], P. De Castro Manzano[a], T. Dorigo[a], U. Dosselli[a], F. Gasparini[a,b], U. Gasparini[a,b], A. Gozzelino[a], S. Lacaprara[a], M. Margoni[a,b], A. T. Meneguzzo[a,b], N. Pozzobon[a,b], P. Ronchese[a,b], R. Rossin[a,b], F. Simonetto[a,b], E. Torassa[a], M. Zanetti[a,b], P. Zotto[a,b], G. Zumerle[a,b]

INFN Sezione di Pavia [a], Università di Pavia [b], Pavia, Italy
A. Braghieri[a], F. Fallavollita[a,b], A. Magnani[a,b], P. Montagna[a,b], S. P. Ratti[a,b], V. Re[a], M. Ressegotti, C. Riccardi[a,b], P. Salvini[a], I. Vai[a,b], P. Vitulo[a,b]

INFN Sezione di Perugia [a], Università di Perugia [b], Perugia, Italy
L. Alunni Solestizi[a,b], G. M. Bilei[a], D. Ciangottini[a,b], L. Fanò[a,b], P. Lariccia[a,b], R. Leonardi[a,b], G. Mantovani[a,b], V. Mariani[a,b], M. Menichelli[a], A. Saha[a], A. Santocchia[a,b], D. Spiga

INFN Sezione di Pisa [a], Università di Pisa [b], Scuola Normale Superiore di Pisa [c], Pisa, Italy
K. Androsov[a], P. Azzurri[a,12], G. Bagliesi[a], J. Bernardini[a], T. Boccali[a], L. Borrello, R. Castaldi[a], M. A. Ciocci[a,b], R. Dell'Orso[a], G. Fedi[a], L. Giannini[a,c], A. Giassi[a], M. T. Grippo[a,26], F. Ligabue[a,c], T. Lomtadze[a], E. Manca[a,c], G. Mandorli[a,c], L. Martini[a,b], A. Messineo[a,b], F. Palla[a], A. Rizzi[a,b], A. Savoy-Navarro[a,28], P. Spagnolo[a], R. Tenchini[a], G. Tonelli[a,b], A. Venturi[a], P. G. Verdini[a]

INFN Sezione di Roma [a], Università di Roma [b], Rome, Italy
L. Barone[a,b], F. Cavallari[a], M. Cipriani[a,b], D. Del Re[a,b,12], M. Diemoz[a], S. Gelli[a,b], E. Longo[a,b], F. Margaroli[a,b], B. Marzocchi[a,b], P. Meridiani[a], G. Organtini[a,b], R. Paramatti[a,b], F. Preiato[a,b], S. Rahatlou[a,b], C. Rovelli[a], F. Santanastasio[a,b]

INFN Sezione di Torino [a], Università di Torino [b], Torino, Italy, Università del Piemonte Orientale [c], Novara, Italy
N. Amapane[a,b], R. Arcidiacono[a,c,12], S. Argiro[a,b], M. Arneodo[a,c], N. Bartosik[a], R. Bellan[a,b], C. Biino[a], N. Cartiglia[a], F. Cenna[a,b], M. Costa[a,b], R. Covarelli[a,b], A. Degano[a,b], N. Demaria[a], B. Kiani[a,b], C. Mariotti[a], S. Maselli[a], E. Migliore[a,b], V. Monaco[a,b], E. Monteil[a,b], M. Monteno[a], M. M. Obertino[a,b], L. Pacher[a,b], N. Pastrone[a], M. Pelliccioni[a], G. L. Pinna Angioni[a,b], F. Ravera[a,b], A. Romero[a,b], M. Ruspa[a,c], R. Sacchi[a,b], K. Shchelina[a,b], V. Sola[a], A. Solano[a,b], A. Staiano[a], P. Traczyk[a,b]

INFN Sezione di Trieste [a], Università di Trieste [b], Trieste, Italy
S. Belforte[a], M. Casarsa[a], F. Cossutti[a], G. Della Ricca[a,b], A. Zanetti[a]

Kyungpook National University, Taegu, Korea
D. H. Kim, G. N. Kim, M. S. Kim, J. Lee, S. Lee, S. W. Lee, Y. D. Oh, S. Sekmen, D. C. Son, Y. C. Yang

Chonbuk National University, Chonju, Korea
A. Lee

Chonnam National University, Institute for Universe and Elementary Particles, Kwangju, Korea
H. Kim, D. H. Moon, G. Oh

Hanyang University, Seoul, Korea
J. A. Brochero Cifuentes, J. Goh, T. J. Kim

Korea University, Seoul, Korea
S. Cho, S. Choi, Y. Go, D. Gyun, S. Ha, B. Hong, Y. Jo, Y. Kim, K. Lee, K. S. Lee, S. Lee, J. Lim, S. K. Park, Y. Roh

Seoul National University, Seoul, Korea
J. Almond, J. Kim, J. S. Kim, H. Lee, K. Lee, K. Nam, S. B. Oh, B. C. Radburn-Smith, S. h. Seo, U. K. Yang, H. D. Yoo, G. B. Yu

University of Seoul, Seoul, Korea
M. Choi, H. Kim, J. H. Kim, J. S. H. Lee, I. C. Park, G. Ryu

Sungkyunkwan University, Suwon, Korea
Y. Choi, C. Hwang, J. Lee, I. Yu

Vilnius University, Vilnius, Lithuania
V. Dudenas, A. Juodagalvis, J. Vaitkus

National Centre for Particle Physics, Universiti Malaya, Kuala Lumpur, Malaysia
I. Ahmed, Z. A. Ibrahim, M. A. B. Md Ali[29], F. Mohamad Idris[30], W. A. T. Wan Abdullah, M. N. Yusli, Z. Zolkapli

Centro de Investigacion y de Estudios Avanzados del IPN, Mexico City, Mexico
H. Castilla-Valdez, E. De La Cruz-Burelo, I. Heredia-De La Cruz[31], R. Lopez-Fernandez, J. Mejia Guisao, A. Sanchez-Hernandez

Universidad Iberoamericana, Mexico City, Mexico
S. Carrillo Moreno, C. Oropeza Barrera, F. Vazquez Valencia

Benemerita Universidad Autonoma de Puebla, Puebla, Mexico
I. Pedraza, H. A. Salazar Ibarguen, C. Uribe Estrada

Universidad Autónoma de San Luis Potosí, San Luis Potosí, Mexico
A. Morelos Pineda

University of Auckland, Auckland, New Zealand
D. Krofcheck

University of Canterbury, Christchurch, New Zealand
P. H. Butler

National Centre for Physics, Quaid-I-Azam University, Islamabad, Pakistan
A. Ahmad, M. Ahmad, Q. Hassan, H. R. Hoorani, A. Saddique, M. A. Shah, M. Shoaib, M. Waqas

National Centre for Nuclear Research, Swierk, Poland
H. Bialkowska, M. Bluj, B. Boimska, T. Frueboes, M. Górski, M. Kazana, K. Nawrocki, K. Romanowska-Rybinska, M. Szleper, P. Zalewski

Institute of Experimental Physics, Faculty of Physics, University of Warsaw, Warsaw, Poland
K. Bunkowski, A. Byszuk[32], K. Doroba, A. Kalinowski, M. Konecki, J. Krolikowski, M. Misiura, M. Olszewski, A. Pyskir, M. Walczak

Laboratório de Instrumentação e Física Experimental de Partículas, Lisbon, Portugal
P. Bargassa, C. Beirão Da Cruz Silva, B. Calpas, A. Di Francesco, P. Faccioli, M. Gallinaro, J. Hollar, N. Leonardo, L. Lloret Iglesias, M. V. Nemallapudi, J. Seixas, O. Toldaiev, D. Vadruccio, J. Varela

Joint Institute for Nuclear Research, Dubna, Russia
S. Afanasiev, P. Bunin, M. Gavrilenko, I. Golutvin, I. Gorbunov, A. Kamenev, V. Karjavin, A. Lanev, A. Malakhov, V. Matveev[33,34], V. Palichik, V. Perelygin, S. Shmatov, S. Shulha, N. Skatchkov, V. Smirnov, N. Voytishin, A. Zarubin

Petersburg Nuclear Physics Institute, Gatchina (St. Petersburg), Russia
Y. Ivanov, V. Kim[35], E. Kuznetsova[36], P. Levchenko, V. Murzin, V. Oreshkin, I. Smirnov, V. Sulimov, L. Uvarov, S. Vavilov, A. Vorobyev

Institute for Nuclear Research, Moscow, Russia
Yu. Andreev, A. Dermenev, S. Gninenko, N. Golubev, A. Karneyeu, M. Kirsanov, N. Krasnikov, A. Pashenkov, D. Tlisov, A. Toropin

Institute for Theoretical and Experimental Physics, Moscow, Russia
V. Epshteyn, V. Gavrilov, N. Lychkovskaya, V. Popov, I. Pozdnyakov, G. Safronov, A. Spiridonov, A. Stepennov, M. Toms, E. Vlasov, A. Zhokin

Moscow Institute of Physics and Technology, Moscow, Russia
T. Aushev, A. Bylinkin[34]

National Research Nuclear University 'Moscow Engineering Physics Institute' (MEPhI), Moscow, Russia
R. Chistov[37], M. Danilov[37], P. Parygin, D. Philippov, S. Polikarpov, E. Tarkovskii

P.N. Lebedev Physical Institute, Moscow, Russia
V. Andreev, M. Azarkin[34], I. Dremin[34], M. Kirakosyan[34], A. Terkulov

Skobeltsyn Institute of Nuclear Physics, Lomonosov Moscow State University, Moscow, Russia
A. Baskakov, A. Belyaev, E. Boos, M. Dubinin[38], L. Dudko, A. Ershov, A. Gribushin, V. Klyukhin, O. Kodolova, I. Lokhtin, I. Miagkov, S. Obraztsov, S. Petrushanko, V. Savrin, A. Snigirev

Novosibirsk State University (NSU), Novosibirsk, Russia
V. Blinov[39], Y. Skovpen[39], D. Shtol[39]

State Research Center of Russian Federation, Institute for High Energy Physics, Protvino, Russia
I. Azhgirey, I. Bayshev, S. Bitioukov, D. Elumakhov, V. Kachanov, A. Kalinin, D. Konstantinov, V. Krychkine, V. Petrov, R. Ryutin, A. Sobol, S. Troshin, N. Tyurin, A. Uzunian, A. Volkov

University of Belgrade, Faculty of Physics and Vinca Institute of Nuclear Sciences, Belgrade, Serbia
P. Adzic[40], P. Cirkovic, D. Devetak, M. Dordevic, J. Milosevic, V. Rekovic

Centro de Investigaciones Energéticas Medioambientales y Tecnológicas (CIEMAT), Madrid, Spain
J. Alcaraz Maestre, M. Barrio Luna, M. Cerrada, N. Colino, B. De La Cruz, A. Delgado Peris, A. Escalante Del Valle, C. Fernandez Bedoya, J. P. Fernández Ramos, J. Flix, M. C. Fouz, P. Garcia-Abia, O. Gonzalez Lopez, S. Goy Lopez, J. M. Hernandez, M. I. Josa, A. Pérez-Calero Yzquierdo, J. Puerta Pelayo, A. Quintario Olmeda, I. Redondo, L. Romero, M. S. Soares, A. lvarez Fernández

Universidad Autónoma de Madrid, Madrid, Spain
J. F. de Trocóniz, M. Missiroli, D. Moran

Universidad de Oviedo, Oviedo, Spain
J. Cuevas, C. Erice, J. Fernandez Menendez, I. Gonzalez Caballero, J. R. González Fernández, E. Palencia Cortezon, S. Sanchez Cruz, I. Suárez Andrés, P. Vischia, J. M. Vizan Garcia

Instituto de Física de Cantabria (IFCA), CSIC-Universidad de Cantabria, Santander, Spain
I. J. Cabrillo, A. Calderon, B. Chazin Quero, E. Curras, M. Fernandez, J. Garcia-Ferrero, G. Gomez, A. Lopez Virto, J. Marco, C. Martinez Rivero, P. Martinez Ruiz del Arbol, F. Matorras, J. Piedra Gomez, T. Rodrigo, A. Ruiz-Jimeno, L. Scodellaro, N. Trevisani, I. Vila, R. Vilar Cortabitarte

CERN, European Organization for Nuclear Research, Geneva, Switzerland
D. Abbaneo, E. Auffray, P. Baillon, A. H. Ball, D. Barney, M. Bianco, P. Bloch, A. Bocci, C. Botta, T. Camporesi, R. Castello, M. Cepeda, G. Cerminara, E. Chapon, Y. Chen, D. d'Enterria, A. Dabrowski, V. Daponte, A. David, M. De Gruttola, A. De Roeck, E. Di Marco[41], M. Dobson, B. Dorney, T. du Pree, M. Dünser, N. Dupont, A. Elliott-Peisert, P. Everaerts, G. Franzoni, J. Fulcher, W. Funk, D. Gigi, K. Gill, F. Glege, D. Gulhan, S. Gundacker, M. Guthoff, P. Harris, J. Hegeman, V. Innocente, P. Janot, O. Karacheban[15], J. Kieseler, H. Kirschenmann, V. Knünz, A. Kornmayer[12], M. J. Kortelainen, C. Lange, P. Lecoq, C. Lourenço, M. T. Lucchini, L. Malgeri, M. Mannelli, A. Martelli, F. Meijers, J. A. Merlin, S. Mersi, E. Meschi, P. Milenovic[42], F. Moortgat, M. Mulders, H. Neugebauer, S. Orfanelli, L. Orsini, L. Pape, E. Perez, M. Peruzzi, A. Petrilli, G. Petrucciani, A. Pfeiffer, M. Pierini, A. Racz, T. Reis, G. Rolandi[43], M. Rovere, H. Sakulin, C. Schäfer, C. Schwick, M. Seidel, M. Selvaggi, A. Sharma, P. Silva, P. Sphicas[44], J. Steggemann, M. Stoye, M. Tosi, D. Treille, A. Triossi, A. Tsirou, V. Veckalns[45], G. I. Veres[17], M. Verweij, N. Wardle, W. D. Zeuner

Paul Scherrer Institut, Villigen, Switzerland
W. Bertl[†], K. Deiters, W. Erdmann, R. Horisberger, Q. Ingram, H. C. Kaestli, D. Kotlinski, U. Langenegger, T. Rohe, S. A. Wiederkehr

Institute for Particle Physics, ETH Zurich, Zurich, Switzerland
F. Bachmair, L. Bäni, P. Berger, L. Bianchini, B. Casal, G. Dissertori, M. Dittmar, M. Donegà, C. Grab, C. Heidegger, D. Hits, J. Hoss, G. Kasieczka, T. Klijnsma, W. Lustermann, B. Mangano, M. Marionneau, M. T. Meinhard, D. Meister, F. Micheli, P. Musella, F. Nessi-Tedaldi, F. Pandolfi, J. Pata, F. Pauss, G. Perrin, L. Perrozzi, M. Quittnat, M. Rossini, M. Schönenberger, L. Shchutska, A. Starodumov[46], V. R. Tavolaro, K. Theofilatos, M. L. Vesterbacka Olsson, R. Wallny, A. Zagozdzinska[32], D. H. Zhu

Universität Zürich, Zurich, Switzerland
T. K. Aarrestad, C. Amsler[47], L. Caminada, M. F. Canelli, A. De Cosa, S. Donato, C. Galloni, A. Hinzmann, T. Hreus, B. Kilminster, J. Ngadiuba, D. Pinna, G. Rauco, P. Robmann, D. Salerno, C. Seitz, A. Zucchetta

National Central University, Chung-Li, Taiwan
V. Candelise, T. H. Doan, Sh. Jain, R. Khurana, M. Konyushikhin, C. M. Kuo, W. Lin, A. Pozdnyakov, S. S. Yu

National Taiwan University (NTU), Taipei, Taiwan
Arun Kumar, P. Chang, Y. Chao, K. F. Chen, P. H. Chen, F. Fiori, W.-S. Hou, Y. Hsiung, Y. F. Liu, R.-S. Lu, M. Miñano Moya, E. Paganis, A. Psallidas, J. F. Tsai

Chulalongkorn University, Faculty of Science, Department of Physics, Bangkok, Thailand
B. Asavapibhop, K. Kovitanggoon, G. Singh, N. Srimanobhas

Cukurova University, Physics Department, Science and Art Faculty, Adana, Turkey
A. Adiguzel[48], F. Boran, S. Cerci[49], S. Damarseckin, Z. S. Demiroglu, C. Dozen, I. Dumanoglu, S. Girgis, G. Gokbulut, Y. Guler, I. Hos[50], E. E. Kangal[51], O. Kara, U. Kiminsu, M. Oglakci, G. Onengut[52], K. Ozdemir[53], D. Sunar Cerci[49], B. Tali[49], H. Topakli[54], S. Turkcapar, I. S. Zorbakir, C. Zorbilmez

Middle East Technical University, Physics Department, Ankara, Turkey
B. Bilin, G. Karapinar[55], K. Ocalan[56], M. Yalvac, M. Zeyrek

Bogazici University, Istanbul, Turkey
E. Gülmez, M. Kaya[57], O. Kaya[58], S. Tekten, E. A. Yetkin[59]

Istanbul Technical University, Istanbul, Turkey
M. N. Agaras, S. Atay, A. Cakir, K. Cankocak

Institute for Scintillation Materials of National Academy of Science of Ukraine, Kharkov, Ukraine
B. Grynyov

National Scientific Center, Kharkov Institute of Physics and Technology, Kharkov, Ukraine
L. Levchuk, P. Sorokin

University of Bristol, Bristol, UK
R. Aggleton, F. Ball, L. Beck, J. J. Brooke, D. Burns, E. Clement, D. Cussans, H. Flacher, J. Goldstein, M. Grimes, G. P. Heath, H. F. Heath, J. Jacob, L. Kreczko, C. Lucas, D. M. Newbold[60], S. Paramesvaran, A. Poll, T. Sakuma, S. Seif El Nasr-storey, D. Smith, V. J. Smith

Rutherford Appleton Laboratory, Didcot, UK
K. W. Bell, A. Belyaev[61], C. Brew, R. M. Brown, L. Calligaris, D. Cieri, D. J. A. Cockerill, J. A. Coughlan, K. Harder, S. Harper, E. Olaiya, D. Petyt, C. H. Shepherd-Themistocleous, A. Thea, I. R. Tomalin, T. Williams

Imperial College, London, UK
M. Baber, R. Bainbridge, S. Breeze, O. Buchmuller, A. Bundock, S. Casasso, M. Citron, D. Colling, L. Corpe, P. Dauncey, G. Davies, A. De Wit, M. Della Negra, R. Di Maria, P. Dunne, A. Elwood, D. Futyan, Y. Haddad, G. Hall, G. Iles, T. James, R. Lane, C. Laner, L. Lyons, A.-M. Magnan, S. Malik, L. Mastrolorenzo, T. Matsushita, J. Nash, A. Nikitenko[46], J. Pela, M. Pesaresi, D. M. Raymond, A. Richards, A. Rose, E. Scott, C. Seez, A. Shtipliyski, S. Summers, A. Tapper, K. Uchida, M. Vazquez Acosta[62], T. Virdee[12], D. Winterbottom, J. Wright, S. C. Zenz

Brunel University, Uxbridge, UK
J. E. Cole, P. R. Hobson, A. Khan, P. Kyberd, I. D. Reid, P. Symonds, L. Teodorescu, M. Turner

Baylor University, Waco, USA
A. Borzou, K. Call, J. Dittmann, K. Hatakeyama, H. Liu, N. Pastika

Catholic University of America, Washington, USA
R. Bartek, A. Dominguez

The University of Alabama, Tuscaloosa, USA
A. Buccilli, S. I. Cooper, C. Henderson, P. Rumerio, C. West

Boston University, Boston, USA
D. Arcaro, A. Avetisyan, T. Bose, D. Gastler, D. Rankin, C. Richardson, J. Rohlf, L. Sulak, D. Zou

Brown University, Providence, USA
G. Benelli, D. Cutts, A. Garabedian, J. Hakala, U. Heintz, J. M. Hogan, K. H. M. Kwok, E. Laird, G. Landsberg, Z. Mao, M. Narain, S. Piperov, S. Sagir, R. Syarif, D. Yu

University of California, Davis, Davis, USA
R. Band, C. Brainerd, D. Burns, M. Calderon De La Barca Sanchez, M. Chertok, J. Conway, R. Conway, P. T. Cox, R. Erbacher, C. Flores, G. Funk, M. Gardner, W. Ko, R. Lander, C. Mclean, M. Mulhearn, D. Pellett, J. Pilot, S. Shalhout, M. Shi, J. Smith, M. Squires, D. Stolp, K. Tos, M. Tripathi, Z. Wang

University of California, Los Angeles, USA
M. Bachtis, C. Bravo, R. Cousins, A. Dasgupta, A. Florent, J. Hauser, M. Ignatenko, N. Mccoll, D. Saltzberg, C. Schnaible, V. Valuev

University of California, Riverside, Riverside, USA
E. Bouvier, K. Burt, R. Clare, J. Ellison, J. W. Gary, S. M. A. Ghiasi Shirazi, G. Hanson, J. Heilman, P. Jandir, E. Kennedy, F. Lacroix, O. R. Long, M. Olmedo Negrete, M. I. Paneva, A. Shrinivas, W. Si, H. Wei, S. Wimpenny, B. R. Yates

University of California, San Diego, La Jolla, USA
J. G. Branson, S. Cittolin, M. Derdzinski, B. Hashemi, A. Holzner, D. Klein, G. Kole, V. Krutelyov, J. Letts, I. Macneill, M. Masciovecchio, D. Olivito, S. Padhi, M. Pieri, M. Sani, V. Sharma, S. Simon, M. Tadel, A. Vartak, S. Wasserbaech[63], J. Wood, F. Würthwein, A. Yagil, G. Zevi Della Porta

University of California, Santa Barbara - Department of Physics, Santa Barbara, USA
N. Amin, R. Bhandari, J. Bradmiller-Feld, C. Campagnari, A. Dishaw, V. Dutta, M. Franco Sevilla, C. George, F. Golf, L. Gouskos, J. Gran, R. Heller, J. Incandela, S. D. Mullin, A. Ovcharova, H. Qu, J. Richman, D. Stuart, I. Suarez, J. Yoo

California Institute of Technology, Pasadena, USA
D. Anderson, J. Bendavid, A. Bornheim, J. M. Lawhorn, H. B. Newman, T. Nguyen, C. Pena, M. Spiropulu, J. R. Vlimant, S. Xie, Z. Zhang, R. Y. Zhu

Carnegie Mellon University, Pittsburgh, USA
M. B. Andrews, T. Ferguson, T. Mudholkar, M. Paulini, J. Russ, M. Sun, H. Vogel, I. Vorobiev, M. Weinberg

University of Colorado Boulder, Boulder, USA
J. P. Cumalat, W. T. Ford, F. Jensen, A. Johnson, M. Krohn, S. Leontsinis, T. Mulholland, K. Stenson, S. R. Wagner

Cornell University, Ithaca, USA
J. Alexander, J. Chaves, J. Chu, S. Dittmer, K. Mcdermott, N. Mirman, J. R. Patterson, A. Rinkevicius, A. Ryd, L. Skinnari, L. Soffi, S. M. Tan, Z. Tao, J. Thom, J. Tucker, P. Wittich, M. Zientek

Fermi National Accelerator Laboratory, Batavia, USA
S. Abdullin, M. Albrow, G. Apollinari, A. Apresyan, A. Apyan, S. Banerjee, L. A. T. Bauerdick, A. Beretvas, J. Berryhill, P. C. Bhat, G. Bolla, K. Burkett, J. N. Butler, A. Canepa, G. B. Cerati, H. W. K. Cheung, F. Chlebana, M. Cremonesi, J. Duarte, V. D. Elvira, J. Freeman, Z. Gecse, E. Gottschalk, L. Gray, D. Green, S. Grünendahl, O. Gutsche, R. M. Harris, S. Hasegawa, J. Hirschauer, Z. Hu, B. Jayatilaka, S. Jindariani, M. Johnson, U. Joshi, B. Klima, B. Kreis, S. Lammel, D. Lincoln, R. Lipton, M. Liu, T. Liu, R. Lopes De Sá, J. Lykken, K. Maeshima, N. Magini, J. M. Marraffino, S. Maruyama, D. Mason, P. McBride, P. Merkel, S. Mrenna, S. Nahn, V. O'Dell, K. Pedro, O. Prokofyev, G. Rakness, L. Ristori, B. Schneider, E. Sexton-Kennedy, A. Soha, W. J. Spalding, L. Spiegel, S. Stoynev, J. Strait, N. Strobbe, L. Taylor, S. Tkaczyk, N. V. Tran, L. Uplegger, E. W. Vaandering, C. Vernieri, M. Verzocchi, R. Vidal, M. Wang, H. A. Weber, A. Whitbeck

University of Florida, Gainesville, USA
D. Acosta, P. Avery, P. Bortignon, A. Brinkerhoff, A. Carnes, M. Carver, D. Curry, S. Das, R. D. Field, I. K. Furic, J. Konigsberg, A. Korytov, K. Kotov, P. Ma, K. Matchev, H. Mei, G. Mitselmakher, D. Rank, D. Sperka, N. Terentyev, L. Thomas, J. Wang, S. Wang, J. Yelton

Florida International University, Miami, USA
Y. R. Joshi, S. Linn, P. Markowitz, G. Martinez, J. L. Rodriguez

Florida State University, Tallahassee, USA
A. Ackert, T. Adams, A. Askew, S. Hagopian, V. Hagopian, K. F. Johnson, T. Kolberg, T. Perry, H. Prosper, A. Santra, R. Yohay

Florida Institute of Technology, Melbourne, USA
M. M. Baarmand, V. Bhopatkar, S. Colafranceschi, M. Hohlmann, D. Noonan, T. Roy, F. Yumiceva

University of Illinois at Chicago (UIC), Chicago, USA
M. R. Adams, L. Apanasevich, D. Berry, R. R. Betts, R. Cavanaugh, X. Chen, O. Evdokimov, C. E. Gerber, D. A. Hangal, D. J. Hofman, K. Jung, J. Kamin, I. D. Sandoval Gonzalez, M. B. Tonjes, H. Trauger, N. Varelas, H. Wang, Z. Wu, J. Zhang

The University of Iowa, Iowa City, USA
B. Bilki[64], W. Clarida, K. Dilsiz[65], S. Durgut, R. P. Gandrajula, M. Haytmyradov, V. Khristenko, J.-P. Merlo, H. Mermerkaya[66], A. Mestvirishvili, A. Moeller, J. Nachtman, H. Ogul[67], Y. Onel, F. Ozok[68], A. Penzo, C. Snyder, E. Tiras, J. Wetzel, K. Yi

Johns Hopkins University, Baltimore, USA
B. Blumenfeld, A. Cocoros, N. Eminizer, D. Fehling, L. Feng, A. V. Gritsan, P. Maksimovic, J. Roskes, U. Sarica, M. Swartz, M. Xiao, C. You

The University of Kansas, Lawrence, USA
A. Al-bataineh, P. Baringer, A. Bean, S. Boren, J. Bowen, J. Castle, S. Khalil, A. Kropivnitskaya, D. Majumder, W. Mcbrayer, M. Murray, C. Royon, S. Sanders, E. Schmitz, R. Stringer, J. D. Tapia Takaki, Q. Wang

Kansas State University, Manhattan, USA
A. Ivanov, K. Kaadze, Y. Maravin, A. Mohammadi, L. K. Saini, N. Skhirtladze, S. Toda

Lawrence Livermore National Laboratory, Livermore, USA
F. Rebassoo, D. Wright

University of Maryland, College Park, USA
C. Anelli, A. Baden, O. Baron, A. Belloni, B. Calvert, S. C. Eno, C. Ferraioli, N. J. Hadley, S. Jabeen, G. Y. Jeng, R. G. Kellogg, J. Kunkle, A. C. Mignerey, F. Ricci-Tam, Y. H. Shin, A. Skuja, S. C. Tonwar

Massachusetts Institute of Technology, Cambridge, USA
D. Abercrombie, B. Allen, V. Azzolini, R. Barbieri, A. Baty, R. Bi, S. Brandt, W. Busza, I. A. Cali, M. D'Alfonso, Z. Demiragli, G. Gomez Ceballos, M. Goncharov, D. Hsu, Y. Iiyama, G. M. Innocenti, M. Klute, D. Kovalskyi, Y. S. Lai, Y.-J. Lee, A. Levin, P. D. Luckey, B. Maier, A. C. Marini, C. Mcginn, C. Mironov, S. Narayanan, X. Niu, C. Paus, C. Roland, G. Roland, J. Salfeld-Nebgen, G. S. F. Stephans, K. Tatar, D. Velicanu, J. Wang, T. W. Wang, B. Wyslouch

University of Minnesota, Minneapolis, USA
A. C. Benvenuti, R. M. Chatterjee, A. Evans, P. Hansen, S. Kalafut, Y. Kubota, Z. Lesko, J. Mans, S. Nourbakhsh, N. Ruckstuhl, R. Rusack, J. Turkewitz

University of Mississippi, Oxford, USA
J. G. Acosta, S. Oliveros

University of Nebraska-Lincoln, Lincoln, USA
E. Avdeeva, K. Bloom, D. R. Claes, C. Fangmeier, R. Gonzalez Suarez, R. Kamalieddin, I. Kravchenko, J. Monroy, J. E. Siado, G. R. Snow, B. Stieger

State University of New York at Buffalo, Buffalo, USA
M. Alyari, J. Dolen, A. Godshalk, C. Harrington, I. Iashvili, D. Nguyen, A. Parker, S. Rappoccio, B. Roozbahani

Northeastern University, Boston, USA
G. Alverson, E. Barberis, A. Hortiangtham, A. Massironi, D. M. Morse, D. Nash, T. Orimoto, R. Teixeira De Lima, D. Trocino, R.-J. Wang, D. Wood

Northwestern University, Evanston, USA
S. Bhattacharya, O. Charaf, K. A. Hahn, N. Mucia, N. Odell, B. Pollack, M. H. Schmitt, K. Sung, M. Trovato, M. Velasco

University of Notre Dame, Notre Dame, USA
N. Dev, M. Hildreth, K. Hurtado Anampa, C. Jessop, D. J. Karmgard, N. Kellams, K. Lannon, N. Loukas, N. Marinelli, F. Meng, C. Mueller, Y. Musienko[33], M. Planer, A. Reinsvold, R. Ruchti, G. Smith, S. Taroni, M. Wayne, M. Wolf, A. Woodard

The Ohio State University, Columbus, USA
J. Alimena, L. Antonelli, B. Bylsma, L. S. Durkin, S. Flowers, B. Francis, A. Hart, C. Hill, W. Ji, B. Liu, W. Luo, D. Puigh, B. L. Winer, H. W. Wulsin

Princeton University, Princeton, USA
A. Benaglia, S. Cooperstein, O. Driga, P. Elmer, J. Hardenbrook, P. Hebda, D. Lange, J. Luo, D. Marlow, K. Mei, I. Ojalvo, J. Olsen, C. Palmer, P. Piroué, D. Stickland, A. Svyatkovskiy, C. Tully

University of Puerto Rico, Mayaguez, USA
S. Malik, S. Norberg

Purdue University, West Lafayette, USA
A. Barker, V. E. Barnes, S. Folgueras, L. Gutay, M. K. Jha, M. Jones, A. W. Jung, A. Khatiwada, D. H. Miller, N. Neumeister, J. F. Schulte, J. Sun, F. Wang, W. Xie

Purdue University Northwest, Hammond, USA
T. Cheng, N. Parashar, J. Stupak

Rice University, Houston, USA
A. Adair, B. Akgun, Z. Chen, K. M. Ecklund, F. J. M. Geurts, M. Guilbaud, W. Li, B. Michlin, M. Northup, B. P. Padley, J. Roberts, J. Rorie, Z. Tu, J. Zabel

University of Rochester, Rochester, USA
A. Bodek, P. de Barbaro, R. Demina, Y. t. Duh, T. Ferbel, M. Galanti, A. Garcia-Bellido, J. Han, O. Hindrichs, A. Khukhunaishvili, K. H. Lo, P. Tan, M. Verzetti

The Rockefeller University, New York, USA
R. Ciesielski, K. Goulianos, C. Mesropian

Rutgers, The State University of New Jersey, Piscataway, USA
A. Agapitos, J. P. Chou, Y. Gershtein, T. A. Gómez Espinosa, E. Halkiadakis, M. Heindl, E. Hughes, S. Kaplan, R. Kunnawalkam Elayavalli, S. Kyriacou, A. Lath, R. Montalvo, K. Nash, M. Osherson, H. Saka, S. Salur, S. Schnetzer, D. Sheffield, S. Somalwar, R. Stone, S. Thomas, P. Thomassen, M. Walker

University of Tennessee, Knoxville, USA
M. Foerster, J. Heideman, G. Riley, K. Rose, S. Spanier, K. Thapa

Texas A&M University, College Station, USA
O. Bouhali[69], A. Castaneda Hernandez[69], A. Celik, M. Dalchenko, M. De Mattia, A. Delgado, S. Dildick, R. Eusebi, J. Gilmore, T. Huang, T. Kamon[70], R. Mueller, Y. Pakhotin, R. Patel, A. Perloff, L. Perniè, D. Rathjens, A. Safonov, A. Tatarinov, K. A. Ulmer

Texas Tech University, Lubbock, USA
N. Akchurin, J. Damgov, F. De Guio, P. R. Dudero, J. Faulkner, E. Gurpinar, S. Kunori, K. Lamichhane, S. W. Lee, T. Libeiro, T. Peltola, S. Undleeb, I. Volobouev, Z. Wang

Vanderbilt University, Nashville, USA
S. Greene, A. Gurrola, R. Janjam, W. Johns, C. Maguire, A. Melo, H. Ni, P. Sheldon, S. Tuo, J. Velkovska, Q. Xu

University of Virginia, Charlottesville, USA
M. W. Arenton, P. Barria, B. Cox, R. Hirosky, A. Ledovskoy, H. Li, C. Neu, T. Sinthuprasith, X. Sun, Y. Wang, E. Wolfe, F. Xia

Wayne State University, Detroit, USA
C. Clarke, R. Harr, P. E. Karchin, J. Sturdy, S. Zaleski

University of Wisconsin-Madison, Madison, WI, USA
J. Buchanan, C. Caillol, S. Dasu, L. Dodd, S. Duric, B. Gomber, M. Grothe, M. Herndon, A. Hervé, U. Hussain, P. Klabbers, A. Lanaro, A. Levine, K. Long, R. Loveless, G. A. Pierro, G. Polese, T. Ruggles, A. Savin, N. Smith, W. H. Smith, D. Taylor, N. Woods

† **Deceased**

1: Also at Vienna University of Technology, Vienna, Austria
2: Also at State Key Laboratory of Nuclear Physics and Technology, Peking University, Beijing, China
3: Also at Universidade Estadual de Campinas, Campinas, Brazil
4: Also at Universidade Federal de Pelotas, Pelotas, Brazil
5: Also at Université Libre de Bruxelles, Bruxelles, Belgium
6: Also at Joint Institute for Nuclear Research, Dubna, Russia
7: Also at Suez University, Suez, Egypt
8: Now at British University in Egypt, Cairo, Egypt

9: Now at Helwan University, Cairo, Egypt
10: Also at Université de Haute Alsace, Mulhouse, France
11: Also at Skobeltsyn Institute of Nuclear Physics, Lomonosov Moscow State University, Moscow, Russia
12: Also at CERN, European Organization for Nuclear Research, Geneva, Switzerland
13: Also at RWTH Aachen University, III. Physikalisches Institut A, Aachen, Germany
14: Also at University of Hamburg, Hamburg, Germany
15: Also at Brandenburg University of Technology, Cottbus, Germany
16: Also at Institute of Nuclear Research ATOMKI, Debrecen, Hungary
17: Also at MTA-ELTE Lendület CMS Particle and Nuclear Physics Group, Eötvös Loránd University, Budapest, Hungary
18: Also at Institute of Physics, University of Debrecen, Debrecen, Hungary
19: Also at Indian Institute of Technology Bhubaneswar, Bhubaneswar, India
20: Also at Institute of Physics, Bhubaneswar, India
21: Also at University of Visva-Bharati, Santiniketan, India
22: Also at University of Ruhuna, Matara, Sri Lanka
23: Also at Isfahan University of Technology, Isfahan, Iran
24: Also at Yazd University, Yazd, Iran
25: Also at Plasma Physics Research Center, Science and Research Branch, Islamic Azad University, Tehran, Iran
26: Also at Università degli Studi di Siena, Siena, Italy
27: Also at INFN Sezione di Milano-Bicocca; Università di Milano-Bicocca, Milan, Italy
28: Also at Purdue University, West Lafayette, USA
29: Also at International Islamic University of Malaysia, Kuala Lumpur, Malaysia
30: Also at Malaysian Nuclear Agency, MOSTI, Kajang, Malaysia
31: Also at Consejo Nacional de Ciencia y Tecnología, Mexico City, Mexico
32: Also at Warsaw University of Technology, Institute of Electronic Systems, Warsaw, Poland
33: Also at Institute for Nuclear Research, Moscow, Russia
34: Now at National Research Nuclear University 'Moscow Engineering Physics Institute' (MEPhI), Moscow, Russia
35: Also at St. Petersburg State Polytechnical University, St. Petersburg, Russia
36: Also at University of Florida, Gainesville, USA
37: Also at P.N. Lebedev Physical Institute, Moscow, Russia
38: Also at California Institute of Technology, Pasadena, USA
39: Also at Budker Institute of Nuclear Physics, Novosibirsk, Russia
40: Also at Faculty of Physics, University of Belgrade, Belgrade, Serbia
41: Also at INFN Sezione di Roma; Sapienza Università di Roma, Rome, Italy
42: Also at University of Belgrade, Faculty of Physics and Vinca Institute of Nuclear Sciences, Belgrade, Serbia
43: Also at Scuola Normale e Sezione dell'INFN, Pisa, Italy
44: Also at National and Kapodistrian University of Athens, Athens, Greece
45: Also at Riga Technical University, Riga, Latvia
46: Also at Institute for Theoretical and Experimental Physics, Moscow, Russia
47: Also at Albert Einstein Center for Fundamental Physics, Bern, Switzerland
48: Also at Istanbul University, Faculty of Science, Istanbul, Turkey
49: Also at Adiyaman University, Adiyaman, Turkey
50: Also at Istanbul Aydin University, Istanbul, Turkey
51: Also at Mersin University, Mersin, Turkey
52: Also at Cag University, Mersin, Turkey
53: Also at Piri Reis University, Istanbul, Turkey
54: Also at Gaziosmanpasa University, Tokat, Turkey
55: Also at Izmir Institute of Technology, Izmir, Turkey
56: Also at Necmettin Erbakan University, Konya, Turkey
57: Also at Marmara University, Istanbul, Turkey
58: Also at Kafkas University, Kars, Turkey
59: Also at Istanbul Bilgi University, Istanbul, Turkey
60: Also at Rutherford Appleton Laboratory, Didcot, UK
61: Also at School of Physics and Astronomy, University of Southampton, Southampton, UK

62: Also at Instituto de Astrofísica de Canarias, La Laguna, Spain
63: Also at Utah Valley University, Orem, USA
64: Also at BEYKENT UNIVERSITY, Istanbul, Turkey
65: Also at Bingol University, Bingol, Turkey
66: Also at Erzincan University, Erzincan, Turkey
67: Also at Sinop University, Sinop, Turkey
68: Also at Mimar Sinan University, Istanbul, Istanbul, Turkey
69: Also at Texas A&M University at Qatar, Doha, Qatar
70: Also at Kyungpook National University, Taegu, Korea